MASSACHUSETTS INSTITUTE OF TECHNOLOGY

ARTIFICIAL INTELLIGENCE LABORATORY

A. I. memo No. 573/A April, 1980 (updated October, 1981)

A MODEL FOR THE SPATIO - TEMPORAL ORGANIZATION OF X - AND Y - TYPE GANGLION CELLS IN THE PRIMATE RETINA

J. Richter and S. Ullman

Abstract: A model is proposed for the spatial and temporal characteristics of X - and Y - type responses of ganglion cells in the primate retina. The model is related to a theory of directional selectivity proposed by Marr & Ullman [1981]. The X - and Y - type responses predicted by the model to a variety of stimuli are examined and compared with electrophysiological recordings. A number of implications an predictions are discussed.

This report describes research done at the Artificial Intelligence Laboratory of the Massachusetts Institute of Technology. Support for this research was provided in part by National Science Foundation Grant MCS77 - 07569.

Abstract

A model is proposed for the spatial and temporal characteristics of X- and Y-type responses of ganglion cells in the primate retina.

Spatial aspects of the model:

Based on the geometry of the cones, horizontal, and bipolar cells in the outer Plexiform Layer, it is suggested that the spatial organization of the receptive fields may take place at the level of the bipolar cells.

Two sizes of receptive field, both with the shape of a difference-of-gaussians, can be constructed at this level. In the central fovea, one has a central diameter of about 80" (the midget bipolar channel), the second about 150" of arc (the flat diffuse bipolar channel).

The larger receptive fields of Y-units are generated by a convergence of smaller units at the level of the ganglion cells.

Temporal aspects:

The X-type temporal response is determined primarily by the fact that its surround response is slower than, and delayed with respect to, the center response.

The Y-type response is generated in the Inner Plexiform Layer by a derivative-like operation on the bipolar cells signal (taking place in the dyad synaptic structure), followed by a rectification in the convergence of these signals on the ganglion cell.

The X- and Y-type responses predicted by the model, for a variety of stimuli, were examined and compared with available electrophysiological recordings. Finally, certain predictions derived from the model are discussed.

1. Introduction

In this paper, a model for the spatio-temporal organization of receptive fields in the primate retina is proposed. The primary goal of the model is to account for the origin of X- and Y-type responses in retinal ganglion cells.

The paper is organized into four parts. The first part surveys background data regarding the X/Y classification and retinal structure. The second part proposes a model for the generation of X- and Y-type units in the retina. The third part compares the X- and Y-type responses predicted by the model with electro-physiological recordings for a variety of stimuli. The fourth and last part contains a short discussion and summary.

1.1 Spatio-temporal organization of X and Y units

The spatial center-surround organization of retinal ganglion cells was first discovered by Kuffler [1952, 1953]. Rodieck and Stone [1965b] suggested that this organization was the result of superimposing a small central excitatory region on a larger inhibitory "dome" that extends over the entire receptive field. Rodieck [1965] and Enroth-Cugell & Robson [1966] described the two "domes" as gaussians, thus describing the receptive field as a difference of two gaussians (DOG).

In 1966, Enroth-Cugell & Robson suggested a distinction between two classes of retinal ganglion cells in the cat (termed X and Y cells), on the basis of the linearity of their response to alternating gratings. When a grating is turned on and off in the receptive field of an X-type cell, a "null position" at which no response is elicited, can be found. Y-cells, in contrast, have no such null position, and often respond to both the on and the off phase of the stimulation [Hochstein & Shapely, 1976a, cat; Schiller & Malpeli, 1977 De Monasterio, 1978b, monkey]. Following this classification, Cleland, Dubin & Levick [1971] found that responses of both retinal and LGN cells in the cat can be subdivided into sustained and transient response types, and that this classification seems to correlate with the X/Y classification (the linear units being the more sustained ones). similar properties were found by De Monasterio [1978 b] in the monkey.

In addition to the linear/non-linear and sustained/transient distinctions, other parameters were suggested to correlate with the X/Y subdivision. These include:

Size: Y-cells have larger receptive fields (measured in terms of radius of the unit's center) than X-cells at the same retinal eccentricity [Enroth - Cugell & Robson, 1966; Boycott & Wassle, 1974; Peichl & Wassle, 1979, cat; De Monasterio & Gouras, 1975, monkey].

Color specificity: In the monkey X-cells are often cone-specific, while Y-cells tend to have a broad band response [Schiller & Malpeli, 1977; De Monasterio & Gouras 1975; De Monasterio 1978a,b].

Shift and McIlwain effects: are significantly more pronounced in Y-type cells [Cleland, Dubin & Levick, 1971; Barlow, Derrington, Harris & Lennie, 1977, in the cat].

Conduction speed: is higher in outcoming fibers from Y-type ganglion cells, by about 70-100% [Cleland, Dubin & Levick 1971; Dreher, Fukada & Rodieck 1976, in the cat; Sherman et. al. 1976; Schiller & Malpeli 1977, in the monkey].

Anatomy: retinal X and Y cells differ in their anatomical appearance [Boycott & Wassle 1974, in the cat], and in their relative densities at different eccentricities [Cleland & Levick 1974, Fukada & Stone 1974; Wassle, Levick & Cleland 1975; in the cat, De Monasterio & Gouras 1975; De Monasterio, 1978a; in the monkey]. There is evidence suggesting that in the monkey their target cells in the LGN are organized in different layers [Dreher et. al. 1976; Sherman et. al. 1976], which then project to distinct cortical layers [Hubel & Wiesel, 1972]. For a detailed summary of X/Y differences in the cat see also [Rodieck, 1979].

1.2 X/Y properties incorporated in the model

Although not all of the above distinctions are universally accepted as pertaining to X – Y classification, the evidence strongly suggests the existence of sub-populations of retinal cells with different spatio-temporal characteristics. (There are additional cell types in the retina, e.g. the W-cells, [Stone & Hoffmann, 1972; Stone & Fukada, 1974; in the cat, De Monasterio, 1978c; in the monkey] but these will not be considered here.) It appears possible, however, that the X/Y partition may not be sharply defined, for two reasons. First, the

correlation among the various properties that distinguish X- from Y- cells is not ideal. Second, there may exist X and Y cells with intermediate properties, e.g. between pure sustained and pure transient (see, e.g., Schiller & Malpeli, 1977, Fig. 8; De Monasterio, 1978a, Fig. 11). For methodological reasons, however, we shall start by examining "idealized X" and "idealized Y" responses, defined by their transience and linearity. Thus, an idealized X-response would be sustained and linear, while an idealized Y-response would be transient and non-linear. We shall then suggest how intermediate responses may be generated. The receptive field's size and some aspects of color specificity will also be discussed, but the shift and McIlwain effects will not be considered. The model further assumes stable adaptation level in photopic vision, so that the effect of rod mechanisms and adaptation processes (as well as the contrast gain control described by Shapley & Victor, 1978) will not be considered. The main aim of the model is to account for the origin of X- and Y- type responses (subject to the above limitations), and to explicitly predict X- and Y-type responses to arbitrary spatio-temporal patterns.

1.3 Anatomy and Physiology of the vertebrate retina

In this section, aspects of the anatomy and physiology of the vertebrate retina will be briefly reviewed. The review is not intended to be complete, but to provide a general overview and to introduce the data of direct relevance to the model. Since physiological data on the primate retina is restricted primarily to ganglion cells, the model incorporates certain data from the retinae of lower vertebrates. Our strategy in adopting such data will be explained.

1.3.1 Anatomy

Detailed descriptions of the primate retina can be found in the works of [Cajal, 1911; Polyak, 1941; Dowling & Boycott, 1966; Boycott & Dowling, 1969; Kolb, 1970; Boycott & Kolb, 1973]. The general structure of the retina is summarized in Figure 1. The first layer of cells includes the rod and cone photoreceptors. In the outer plexiform layer (OPL), the cones contact the horizontal cells and the invaginating midget bipolar cells in a synaptic structure called the triad, and the flat-midget and flat-diffuse bipolar cells on the basal

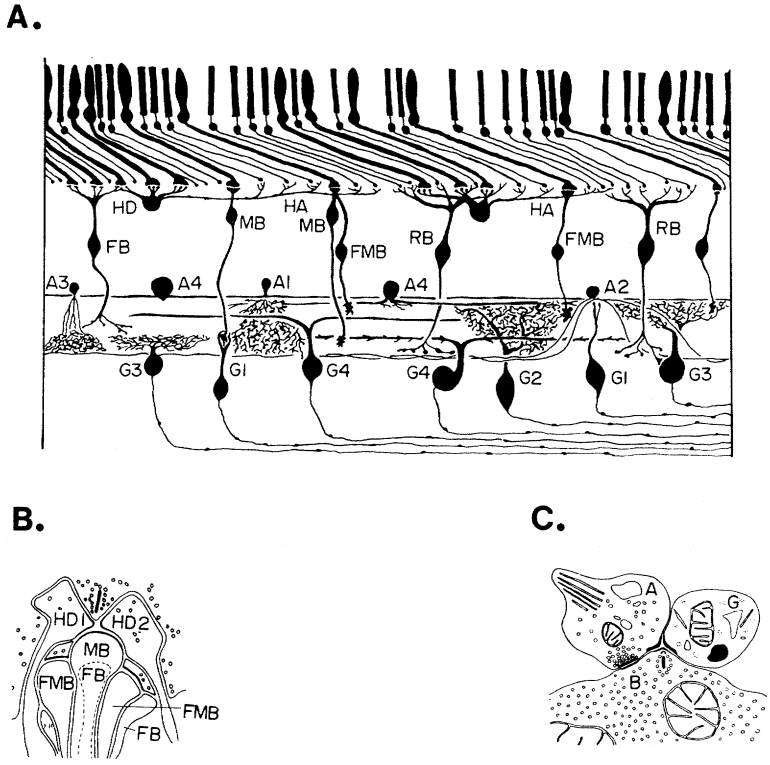

Figure 1. The primate's retina. A: The retinal structure (after Boycott & Dowling 1969, fig. 98) showing the different cell types. The upper row are the receptors, (HD) and (HA) the horizontal cells, (FB) a flat bipolar cell, (MB) an invaginating midget bipolar cell, (FMB) a flat midget bipolar cell, (A1) to (A4) different amacrine cells, (G1) midget ganglion cells and (G4) Y ganglion cells. B: the triad in the cone's pedicle (from Kolb 1970, fig. 59), showing the processes of the horizontal cells (HD1, HD2),the flat bipolar cell (FB) and the midget bipolar cells (MB, FMB). C: the dyad (from Dowling & Boycott 1966, fig. 14) showing the synapses from the bipolar cell(B) to the amacrine cell (A) and to the ganglion cell(G), as well as the reciprocal synapse of the amacrine cell onto the bipolar cell.

membrane nearby (Fig. 1-b). Midget and flat-midget bipolar cells contact a single cone, while the flat–diffuse bipolar cells contact about 6-7 cones. The horizontal cells provide lateral connections in the OPL. Two distinct types of horizontal cells have been described in the primate [Kolb, Mariani & Gallego, 1980]. Type I have a dendritic field diameterof about 20μ in the fovea connecting exclusively to cones, and a larger axonic field connecting exclusively to rods. The two fields are connected by a long, non–branching axon. This connection is likely to be physiologically ineffective [Kolb, Mariani & Gallego, 1980; see also Nelson *et al* regarding type B horizontal cells in the cat]. Type II horizontal cells in the fovea have a larger and more diffuse dendritic field. their axon is shorter and branching, and it bears clusters of terminals connecting to cone pedicles. It is unknown whether the horizontal cells make efferent connections to cones or to bipolar cells. (Connections to bipolar cells have been shown in the mudpuppy, Dowling & Werblin 1969, and to cones in the turtle, Baylor, Fourtes & O'Bryan, 1971.) Also unknown is whether the connections of horizontal and flat bipolar cells to cones is color-specific, and the extent to which horizonatl cells are interconnected.

The bipolars terminate in the inner plexiform layer (IPL) where they contact both amacrine and ganglion cells in the same synaptic structure, shown in Fig. 1-c (This synaptic arrangement is called the *dyad.*) In close proximity to this structure, the amacrine cell synapses back onto the bipolar cell, and it also contacts directly the ganglion cell. There are several anatomically distinct types of amacrine and ganglion cells that differ in the size and shape of their dendritic fields, as illustrated schematically in Fig. 1-a. The IPL is further divided into two layers: invaginating midget bipolar cells terminate in its inner third layer (sublamina b), and flat-midget in the outer third (sublamina a) [Dowling & Boycott 1969]. In other species On–center bipolar cells have been shown to terminate in sublamina a, and off–center in sublamina b [Famiglietti, Kaneko & Tachibana, 1977, carp; Nelson, Famiglietti & Kolb, 1978, cat].

Figure 1 here.

1.3.2 Physiology – the use of lower vertebrates data

Physiological data on the primate retina is limited to ganglion cells [Gouras, 1968, 1969; De Monasterio & Gouras, 1975; Schiller & Malpeli, 1977; De Monasterio, 1978a, 1978b]. Responses of other retinal cells, when

required, had therefore to be inferred from data concerning other mammals and lower vertebrates. Such an inference has to be exercised with care, but in certain instances is supported by the fact that the basic responses of retinal preganglionic cells show strong similarity across species, such as goldfish and catfish [Chan & Naka, 1976; Kaneko, 1970], the mudpuppy [Werblin & Dowling, 1968; Miller & Dacheux, 1976a,b], salamander [Wunk & Werblin, 1979] and turtle [Schwartz, 1973; Marchiafava & Torre, 1978].

Our strategy has been to adopt the response of a given cell only if (i) it isinvariant across species and (ii) it is also consistent with the primate's retinal anatomy. The responses adopted in this way were:

(1) The cone's response to light increments and decrements.

(2) The temporal response of horizontal cells to light increments and decrements.

(3) The concentrically opponent receptive field of bipolar cells. Also supported by preliminary recordings in the monkey (De Monasterio, personal communication).

(4) The amacrine cell relevant to the model is the bistratified type [Cajal, 1911; Polyak, 1941; Boycott & Dowling, 1969]. Its response was taken to be transient on-off response, as described by Werblin & Dowling [1969], mudpuppy; Kaneko [1970], goldfish; Chan & Naka [1976], catfish; Miller & Dacheux [1976a,b], mud-puppy; and Marchiafava & Torre [1978], turtle. Quantitative adjustments of the time scale were made, since lower vertebrate responses are appreciabelly slower than those of high mammals. More detailed descriptions and justifications of these responses will be given in the exposition of the model in Part 2.

1.4 The model in relation to a theory of directional selectivity

A theory of directional selectivity and its use in early visual processing has been proposed recently by Marr & Ullman [1979]. One implication of this theory is that two types of sub-units with different spatio-temporal characteristics are required for the construction of directionally selective units. Spatially, both sub-units have a DOG-shaped receptive field. Temporally, one is sustained, while the response of the other is proportional to the change in (or, more precisely, the temporal derivative of) the response of the sustained unit. Marr & Ullman suggested that X-type units provide the required sustained "building blocks", while

Y-type units provide the required change-sensitive units. Analysis of available recordings from Y-type units has confirmed that for stimuli moving across the retina at moderate speeds, the Y-type response is indeed in close agreement with the temporal derivative of the X-type response [Marr & Ullman, 1979, Fig. 8, this paper, Fig. 15]. For other stimuli, however, (e.g., alternating gratings, a flickering dot at the center-surround boundary, or full-field stimulation), the response of Y-units deviates considerably from the predictions based on the temporal derivative operation. Similarly, under certain stimulations (e.g., full-field, or a flickering dot at the center-surround boundary), X-units deviate significantly from a pure sustained reponse. It is of interest to examine whether these deviations arise naturally in a biological implementation of the two types of units suggested by computational considerations. One goal of the model was therefore to examine the X- and Y-type responses in light of the computational considerations on the one hand, and the known anatomical and physiological data on the other.

2. The Model

The exposition of the model will be divided into two parts: the spatio-temporal organiztion at the outer plexiform layer (Sections 2.1-2.2), and at the inner plexiform layer (2.3-2.5). Although spatial and temporal aspects cannot be dissociated, the emphasis in the OPL is on the spatial organization, and in the IPL on the temporal response.

2.1 Receptive field organization in the OPL

In this section it will be suggested that the DOG-like receptive field organization is formed in the OPL. Two receptive field sizes can be generated at that level, with center sizes in the fovea of approximately 80" and 150" of arc respectively. Temporally, the surround response is slower than, and delayed with respect to, the center response.

An overall antagonistic center-surround organization of the bipolar cell's receptive field has been ob-

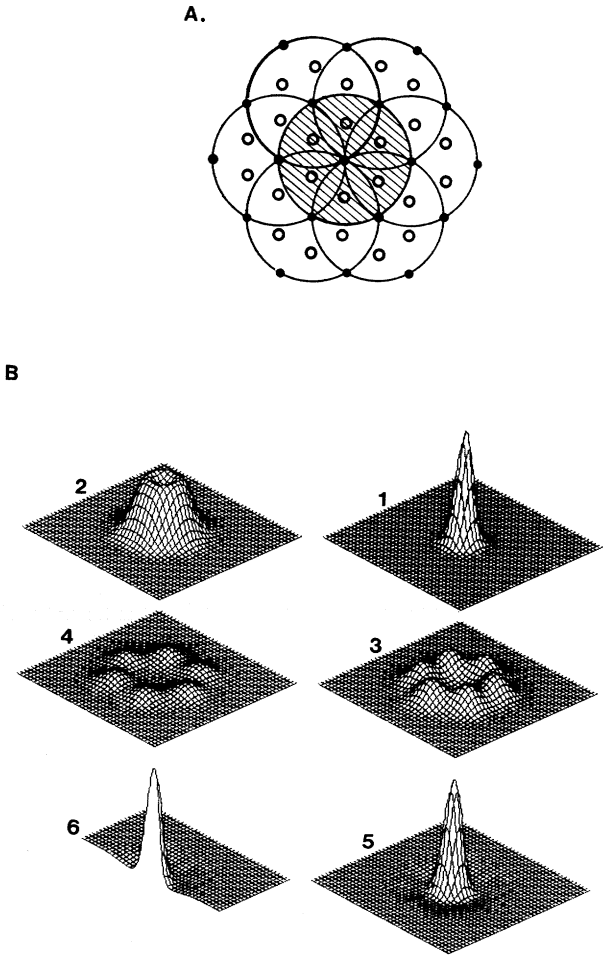

Figure 2. Spatial formation of the receptive field of a midget bipolar cell. The arrengement of cones and horizontal cells is shown in a. Each horizontal cell covers a circle (the shaded area) with a radius three times that of the spacing between cone pedicles (the dots). It contacts seven cones: one in the center and six second order neighbors (filled dots). Thus, seven horizontal cells contact each cone, connecting a total of 19 cones to mediate the surround of a midget bipolr cell (all the filled dots). b. The cotribution to the surround of the central cone and the three concentric "rings" of cones. 1: The contribution of the central cone to its surround. 2, 3, 4: The contributions of the first, second, and third rings. The amplitudes are scaled according to the scaling factor in the model: 7, 4, 2, 1 respectively. The resulting receptive field is shown in 5 and a cut through it in 6.

served in a number of species [Werblin & Dowling, 1969, Werblin, 1970, Norton *et al* , 1970, Kaneko, 1970d, Miller & Dacheux, 1976a, in the mudpuppy; Naka & Nye, 1970, 1971, Naka, Marmarelis & Chan, 1975, in the catfish; Wunk & Werblin, 1979, in the salamander.] Preliminary recordings in the monkey (De Monasterio, personal communication) support this organization. It is unclear, however, whether the final DOG-like shape of the receptive field is generated at this level, and how the different sizes of the X- and Y-type receptive fields are generated. These questions are particularly problematic for the primate retina, since there is no direct physiological data from the primate OPL, and since the organization of primates' OPL may differ from that of lower species, e.g. with respect to horizontal-to-horizontal connections. We shall nevertheless argue that the OPL mechanisms are sufficient to generate DOG-shaped receptive fields of two sizes, one with a center size of about 80" of arc, the other about 150" (in the fovea). The smaller channel is generated by the midget bipolar cells, and the larger by the flat bipolar cells. We shall consider each in turn.

2.1.1 The generation of small DOG-shaped channels by the midget bipolar cells

Midget bipolar cells serve as the inputs to the midget ganglion cells (G1 in Fig. 1), and their center is formed by a single cone [Boycott &Dowling, 1969; Kolb, 1970]. The shape of the center contribution is approximately gaussian with an additional "skirt" [Baylor & Hodgkin, 1973, in the turtle; Nelson 1977, in the cat]. This shape is determined by a combination of the optical properties of the eye [Campbell & Gubish, 1966,Westheimer, 1976] and the optical properties of the cone itself [O'Brian, 1951]. Based on these data the gaussian-like receptive field of a single cone in the human retina has a spatial constant (σ) of about 25" of arc [Marr, Poggio & Hildreth 1981].

The inhibitory surround of the midget bipolars is mediated by the horizontal cells connecting either directly onto the bipolar cells, or back onto the cones [Baylor *et al.*,1971; Naka, 1972; Naka & Witkovsky, 1972]. The spatial shape of this surround contribution would depend on the interconnections that exist among horizontal cells. In the primate retina, effective interconnections among horizontal cells have not been observed [Boycott & Dowling 1969; Kolb, 1970; Boycott & Kolb, 1973], but this may be the result of inade-

quate staining conditions for OPL preparations (Dowling, personal communication.) Some junctions between horizontal cells were observed by Raviola, [1976]. We have therefore considered two different schemes of horizontal interconnections.

In the first scheme, the existence of an electric net created by interconnections among horizontal cells has been assumed. Such interconnections were found in lower vertebrates [Kaneko, 1971; Rodieck, 1973]. The existence of an electric net formed by horizontal cells in the cat (or possibly two networks, formed by the two distinct horizontal cell types) is suggested by the findings of Nelson [1977]. Such an arrangement can provide a good approximation to a given DOG-shaped receptive field, provided that the horizontal cells network has the appropriate space constant. Given the differences in size between the receptive fields in the cat and monkey, the effective space constant of the net should be considerably smaller in the monkey to give the required receptive field shape. Our computation indicated that a space constant of about 20μ would yield a close approximation to a DOG-shape with space constants in the ratio of 1.75. This small space constant is too small for passive conductance in the dendrites themselves but could be the result of the interconnections between the horizontal cells.

In the second scheme, examined in the rest of this section, no horizontal interconnections were assumed. We shall see that a good approximation to a DOG-shape can be obtained in this case as well, by the geometry of the connections among cones, bipolars, and horizontal cells in the primate retina. A possible advantage of this latter arrangement is that it may be superior in preserving cone specificity of the horizontal, and subsequently the bipolar cells.

In the lack of interconnections among horizontal cells, only those cells whose dendritic fields overlaps that of a given bipolar cell can contribute to its surround response. We shall therefore examine the geometrical arrangement of cones and horizontal cells in the primate retina.

The general arrangement of cones in the primate retina approximates a hexagonal packing [e.g. Polyak, 1941; Boycott & Kolb, 1973, Fig. 25 plate 5]. It is possible that the different populations of cones (red, green, blue) are also arranged in a hexagonal pattern [Wassle & Riemann, 1978], as they are in the cyprinid fish

[Scholes, 1975] and the goldfish [Marc & Sperling, 1976], and as has been shown for blue cones in the baboon (Marc & Sperling, 1977). Anatomical data in the monkey suggest that the diameter of type I horizontal cell's dendritic field is about five times larger than the size of the cone pedicle, and that it contacts only a part of the cones within its dendritic field: about 6–9 cones in an area that may contain up to 30 cones (assuming cone density of 220 in $2500\mu^2$ area, and dendritic diameter of 20μ, see Boycott & Kolb, 1973). Light microscopy data [Boycott & Dowling, 1969; Boycott & Kolb, 1973] indicates that the distance between horizontal cells' terminal aggregates (which correspond to their contacts with cone pedicles) is about twice the cone pedicle's diameter. As we shall see, these parameters allow the generation of a DOG–shaped receptive field with the appropriate size for the midget channel (and color specificty of the connections). We have therefore used the parameters of the type I horizontal cells in modelling the midget channel.

From the above studies, the geometrical arrangement of cones and type I horizontal cells in the foveal region of the primate retina can be summarized by the following estimates:

(1) The size of a cone pedicle is about 5μ, and so is the average distance between neighbouring pedicle centers [De Monasterio & Gouras, 1975]. (The diameter of the cone's inner segment, determining its optical collecting area [O'Brian 1951], in the center of the fovea is about $1.5 - 2\ \mu$ and the spacing between neighboring cones is $1.8 - 2.3\ \mu$ [Poliak, 1957]. But at the OPL level the pedicle is the structure that corresponds to one cone.)

(2) The dendritic field diameter of a horizontal cell is about 25μ.

(3) Each horizontal cell contacts about 7 (6-9) cones. The average distance between contacts is about 10μ.

(4) Neighbouring horizontal cells overlap by about 1/2 the diameter of their dendritic fields [Wassle & Riemann, Figs. 5,7].

This geometrical arrangement is diagrammed in Figure 2. The area covered by one horizontal cell is marked by the shaded circle in Fig. 2-A. Within this area, the horizontal cell contacts seven cones: a central one and six others arranged in a concentric ring. Note that this ring is composed not of the six nearest neighbours to the central cone, but of the next six neighbors in the hexagonal arrangement (filled dots in the

shaded area). We shall refer to this second ring as the second-order neighbors of the central cone.

Seven horizontal cells converge in this arrangement on the central cone, connecting a total of 19 cones (the filled dots in Fig. 2-A) to form the surround of the midget channel. The central cone contributes to the surround via seven distinct horizontal cells. The cones in the first, second, and third concentric rings of six cones, each contribute to the surround response via four, two, and a single horizontal cell, respectively (Fig. 2-A). If the relative contribution of each cone to the surround response is roughly proportional to the number of intermediate horizontal cells (i.e., 7, 4, 2, and 1), then a DOG-shaped receptive field will be obtained.

The contribution of the central cone, and of the first, second, and third rings of cones are shown separately in Fig. 2-B, 1-4. The responses are scaled using a weighting of 7,4,2, and 1, respectively. Combined with the center response of a single cone, the receptive field will have the DOG-shape illustrated in Fig. 2-B 5 and 6. The close approximation of the resulting receptive field to a DOG-shape can be seen in Figure 3-a, which compares a projection profile of the receptive field (curve a) with the corresponding profile of a DOG (with space constants in the ratio of 1.75, curve b). (The profile through the simulated receptive field changes slightly as a function of the orientation of the cut through the receptive field. Figure 2(a) shows the maximal deviation from an ideal DOG.) Given the above parameters, the receptive field has a central diameter of about 80" of arc, which is in close agreement with the smallest channel suggested by Marr, Poggio & Hildreth [1981] for human vision.

This spatial model is schematic and idealized, in that it assumes precise packing and interconnections. The resulting similarity between the receptive field and a DOG shape is, however, rather insensitive to the precise parameters. For example, we have examined the receptive field shape with weighting of (12, 9, 2, 1) (rather than 7, 4, 2, 1). This possible modification was suggested by the data in [Kolb, 1970] concerning the number of synapses between cones and horizontal cells. The resulting receptive field was still in good agreement with a two-dimensional DOG. Similarly, changing the number of cones connecting to a horizontal cell between 6 and 9, and introducing some deviation from hexagonal packing, introduce only minor changes in the receptive field shape.

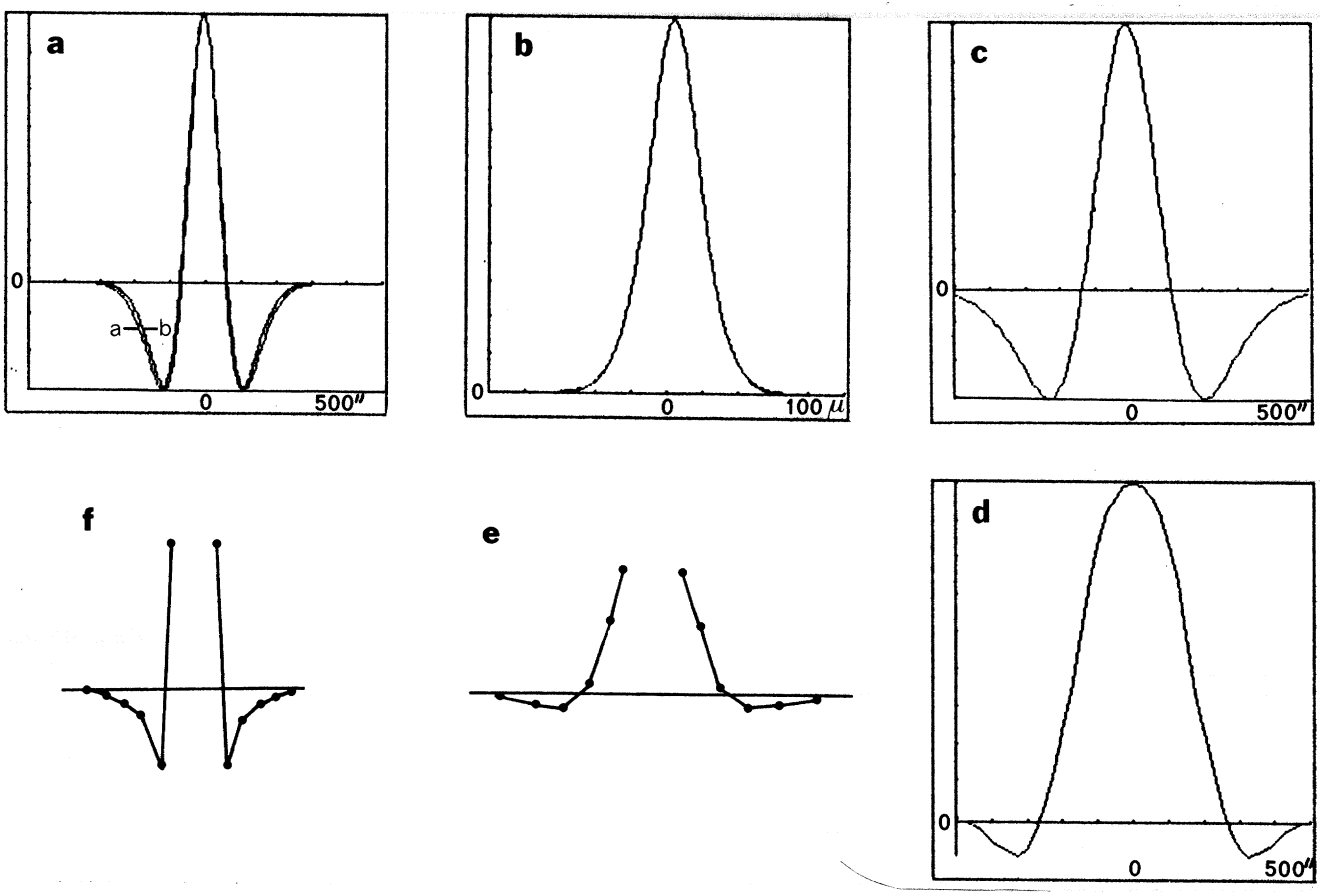

Figure 3. The shape of receptive fields. a. A one-dimensional projection of the receptive field generated under the assumption of no connections between horizontal cells (curve a) is compared to a projection of a difference of gaussians (DOG) with a ratio of 1 : 1.75 between center and surround space constant (curve b). b. The weighting function used for pooling bipolar cells to generate a Y-type ganglion cell (see 2.1.3). c. The resulting receptive Y-type field, obtained by convolving the bipolar receptive field in (a) with the weighting function (b). The result is a ballanced DOG-shaped receptive field twice as wide, and with the same ratio between center and surround space constants, as the original one in (a). d. A simulation of mapping Y-type receptive field with a flickering bar.

The simulation used the ballanced DOG shown in (c). The apparent change in the receptive field shape is due to the temporal differentiation and the different time response characteristics of center and surround mechanisms. e,f, are mappings of Y-type and X- type receptive fields of cat ganglion cells (from [Bullier & Norton 1979 b,]) for comparison with d and a in our simulation.

2.1.2 The receptive field generated by the flat bipolar cell

Flat bipolar cells contact about 6-7 cones each [Boycott & Dowling, 1969; Kolb, 1970; Mariani, 1981], and the distance between their terminal aggregates (where they contact the cone pedicles) is about twice the inter-cone distance [Boycott & Dowling, 1969; Boycott & Kolb, 1973; Mariani, 1981, e.g. plate 4a]. We therefore modeled the flat bipolar cell as connected to a central cone and the ring of its six second-order neighbours, akin to the foveal horizontal cell. The surround of the flat bipolar cell was modeled in the same manner as that of the midget cell. In this case, however, the horizontal cells that contribute to the surround response are those that converge on any of the 6-7 cones forming the center. The resulting receptive field is again closely approximated by a DOG, with a center size of about 150" of arc and space constants in the ratio of about 1.85 (somewhat larger if th surround is mediated by type II horizontal cells.

2.1.3 The generation of larger receptive fields DOG -shaped receptive fields of two sizes can be generated at the OPL level. Larger receptive fields can be generated subsequently by simple convergence. Figure 3-c shows a simulated receptive field, formed by the convergence on a stratified ganglion cell of all the flat bipolar cells whos axons overlap its dendritic field (100 – 200μ, [Boycott & Dowling, 1969]), using the weighing function shown in 3-b. This functin is the sum of four gaussians with space constants of $\sqrt{3}$, $\sqrt{6}$, $\sqrt{9}$ and $\sqrt{12}$. It can be shown that this function will double the size of the receptive field without changing the center -- surround space ratio or ballance. In addition, the feasibility of generating larger receptive fields from smaller ones by convergence alone raises the possibility that larger units can, in principle, also be formed beyond the retinal stage – in the LGN or even the cortex. A word of caution is in order, due to temporal factors, a direct measurment of the spatial organization of the receptive field is difficult to obtain, especially for Y – cells. For example even if the receptive field is a ballanced DOG - shaped receptive field (fig. 3-b) a mapping of the receptive field with flashing spot or bar of light is not expected to reveal such a ballanced DOG. Figure 3-d shows a simulation of the receptive field in 3-b by a flashing bar (the details of the simulation are explained in the next section). Note that the receptive field seems to have an uaballanced shape with a weak surround. Fig.

3-e is a corresponding mapping of a Y–cell in the cat [Bullier & Norton 1979 b, fig. 4].

Conclusion: The foregoing analysis cannot prove, of course, that the generation of DOG - shaped receptive fields is completed in the OPL level. It indicates, however, that given plausible estimates the OPL mechnisms are sufficient for the generation of such DOG - shaped receptive fields, with center diameter of 80" and 150" , in the fovea.

2.2 Temporal aspects of the OPL

The temporal response of bipolar cells is determined by their response to the activity in the cones and the horizontal cells, and by the temporal relation between these two contributions. The temporal responses measured in the bipolar cell to inputs from cones and horizontal cells resemble (disregarding slow adaptation effects) the voltage change across a charging or discharging capacitor (RC circuit) [Norton *et al,* 1968; Werblin & Dowling, 1969; Wunk & Werblin, 1979; in the mudpuppy; Baylor, Fourtes & O'Bryan, 1971; direct measurement from cones and horizontals cells in the turtle]. The time constant of the horizontal cell is, however, longer than that of the cone (about 200 msec. and 100 msec. respectively, in the response to a light increment in the mudpuppy) considerably shorter in mammals. The difference in time constants for the decrement of light appears to be somewhat smaller, but this refinement was not incorporated into our simulations, since at the bipolar cell it does not appear significant.) At the bipolar cell, where the cone and horizontal cell responses are combined, the surround contribution (mediated by the horizontal cells) is delayed with respect to the direct cone contribution by about 20-50 msec. [Miller & Dacheux, 1976a; Werblin, 1977, Fig. 3, in the Mudpuppy; Marchiafava & Torre, 1978, Fig. 5, in the turtle; see also Rodieck, 1973, pp. 443-449]. This delay appears to be caused primarily by the inhibitory synapse of the horizontal cell, since, unlike its inhibitory contribution, the response of the horizontal cell itself does not appear to be delayed appreciably with respect to the cone's [Baylor *et al,* 1971]. Intracellular recordings from cones and horizontal cells in the cat [Nelson, 1977] and from bipolar cells in the monkey [De Monasterio, pesonal communication], indicate a qualitative

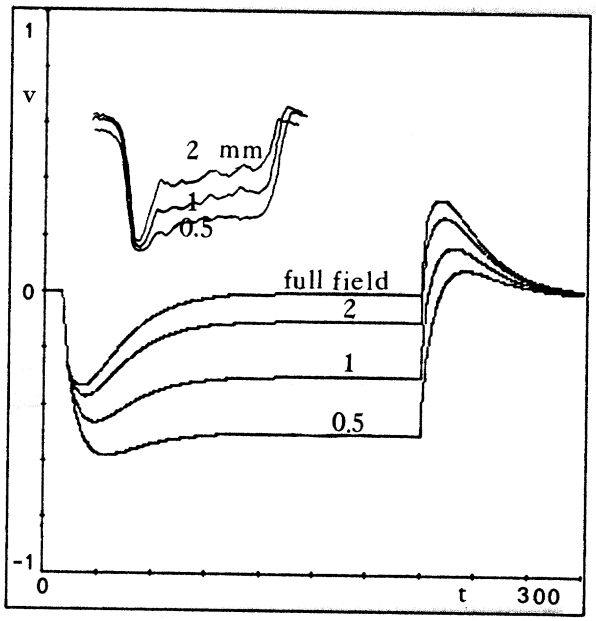

Figure 4. The response of a midget hyperpolarizing bipolar cell as a function of the radius of the stimulating spot. The stimulus is a spot of light turning on and off, and centered on the receptive field. The spot size is expressed in terms of σ, the space constant of the center gaussian. As the radius of the spot is increased from 0.5σ (bottom), to full field (top), the response diminishes in size and becomes more transient due to the increased contribution of the surround mechanism. The inset is from Werblin [1974, fig. 6] for corresponding stimulation conditions, the spot radius given in millimeters. Calibration: Abscissa – time in msec. Ordinate – relative response.The time scale of the inset, recorded in the mudpuppy, is cosiderably slower.

resemblence to lower vertebrates responses, with considerably shorter time constants (factor 5 to 10). Precise estimates of the time constants for higher vertebrates are not available. The parameters incorporated in the model for simulating the temporal aspects of the OPL were time constants of 10 and 20 msec. for the center and surround responses, respectively, and a surround-center delay of 3 msec. The choice of these parameters is justified later by the similarity between the simulated responses of the model, and the recorded ones.

The delay between center and surround responses, and the difference in their respective time constants, introduces transience at the bipolar level. Consider, for instance, the response of a bipolar cell to a small spot of light being turned on in the middle of its receptive field. The center contribution will appear first, followed by the surround contribution that will gradually reduce the combined response to a lower steady-state activity. As the spot increases in size, the response will diminish in size and become more transient. For a full-field illumination (i.e., an increment in uniform illumination across the receptive field), the response will be entirely transient, since after a sufficiently long time the surround response will be equal in magnitude, and opposite in sign, to the center contribution. These expected responses (computed for a DOG with space constants in the ratio of 1.75 and a delay of 3 msec.) are shown in Figure 4 for four sizes of the stimulating dot. The inset is an electrophysiological recording from the mudpuppy by Werblin with slower time scale [1974, Fig. 6]. Similar responses were recently recorded from a limited number of flat diffuse bipolar cells in the rhesus monkey [De Monasterio, personal communication] and their time course is in good agreement with the simulated response in fig. 4.

2.3 The formation of Y-type responses in the IPL

The final spatio-temporal organization of X and Y units is formed in the IPL. The bipolar cells that carry the input to the IPL already have, according to the model, a spatio-temporal organization similar to that of the X-type units. We shall therefore consider first the generation of Y-type responses from the bipolar outputs. We shall argue that the Y-type response is generated in the IPL by a derivative-like operation on the bipolar cells' signal, followed by a rectification in the convergence of these signals on the ganglion cell.

A Y-type response has been characterized as transient. That is, the response follows changes in the light distribution across the unit's receptive field. In the lack of temporal changes, the steady-state activity falls back to the maintained level. This description gives, however, only a partial characterization of the Y-type temporal response; it is insufficient for predicting the response of Y-type units to arbitrary stimuli. We suggest that the primary origin of this transience is a derivative-like operation, probably taking place in the dyad and the reciprocal synapse from the amacrine to the bipolar. The term "derivative-like" means that the operation approximates the temporal derivative of the bipolar cell's signal. A biological system cannot be expected, of course, to perform a precise mathematical differentiation, but for moderate temporal frequencies the operation we suggest can be so approximated.

Support for the derivative-like operation hypothesis comes from three sources. First, in their theory of directional selectivity Marr & Ullman [1980] have observed that for stimuli moving across the retina at moderate speeds the physiological recordings from Y units are in close agreement with the temporal derivative of the corresponding X-type responses. Some of this evidence will be summarized in discussing simulation results in Section 3.6. (see also Spekreijse, 1969, where the notion of phasic ganglion cells as differentiators is suggested explicitly). Second, the anatomy of the dyad appears to have the necessary structure for such a derivative-like operation. In the dyad, the bipolar transmits to the amacrine cell, and the amacrine in turn has a recurrent synapse back onto the bipolar cell in a close spatial proximity to the dyad (usually within 1-3μ [Boycott & Dowling, 1969; Dubin, 1970]). If the recurrent synapse is inhibitory, and if the amplification factors of the synapses are sufficient, a local derivative-like transformation of the signal can be obtained. This effect of the recurrent synapse is illustrated in Figure 5-C. Shown is the computed effect of a recurrent synapse arrangement on the bipolar terminal response. (That is, the ganglion response to the bipolar is obtained by convolving the bipolar signal with the curve in Fig. 5-C). This is a somewhat "smeared out" derivative-like operation, composed of a positive lobe followed by a negative one of longer duration and roughly the same total area. For more detail on this derivative-like operation see Section 4.2.

The third support for the derivative hypothesis comes from the resulting behavior of the model. In

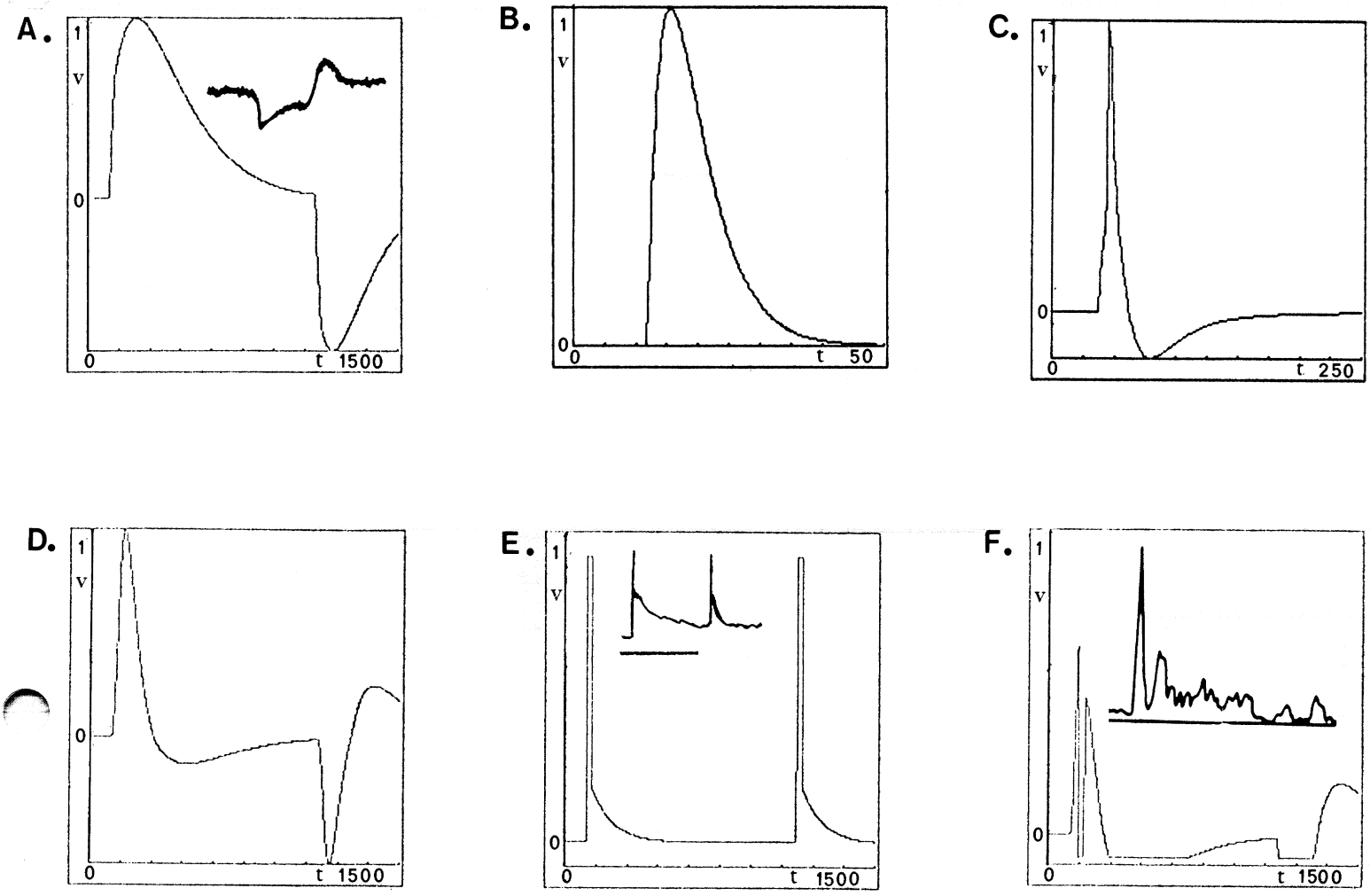

Figure 5. The generation in the model of the Y-response to full field stimulation. A: a depolarizing bipolar cell response, combining a positive cone input (time constant = 10 msec.) and a surround negative input (time constant =20 msec. and delayed by 3 msec.). B: the synaptic time response assumed for the excitatory synapses between the bipolar and the amacrine cell (the alpha function of Jack et. al. [1975]). C: the impulse response of the system between the bipolar and the ganglion cell, combining the cable properties of the bipolar cell, the mechanism of the dyad and the synaptic transmission to the ganglion cell. D: the bipolar signal (A) following the transformation by the dyad (C) and a rectification. E: the Amacrine cell response. It combines contributions of both depolarizing and hyperpolarizing bipolar cells, with spikes superimposed on the slow potential component. F: the final on-center Y-Ganglion cell response.combining the bipolar cell input (D) and the Amacrine input (E) subtracted with a delay. Insets are physiological recordings to demonstrate the similarities between the model and the physiological responses. Inset in A. hyperpolarizing Bipolar [Kaneko 1970]. Inset in E. Amacrine cell [Miller & Dacheux 1976 b, fig. 3]. Inset in F. from monkey's Y-Ganglion cell [De Monasterio 1978 a, fig. 2] Calibration : Abscissa - time in milliseconds, Ordinate - relative response for all the graphs. The on period in A, D, E and F is from 50 to 550 msec.

examining the simulation results, we shall see that the predicted Y-type response agrees closely with the empirical data for a range of different stimuli, thus lending support to the derivative assumption incorporated in the model.

In summary, we suggest that a derivative-like transformation takes place in the IPL. This operation is possible, given the synaptic structure of the IPL, and can account for temporal aspects of the Y-type response. The most plausible candidate for a differentiator is the reciprocal synaptic arrangement in the dyad (analysed in section 4.2), although alternative schemes cannot be completely excluded. This view is supported in part by a recent and independent findings by Shapely & Victor [in preparation] where the best fit for the high pass temporal response of Y– cells was obtained by a low pass feedback mechanism.(This transient response which is generated at the bipolar terminals is expected to have only a small effect on the potential in the bipolar soma, and therefore the soma potential is expected to remain essentialy sustained.)

The bipolar signal transformed by the derivative-like operation is transmitted in the dyad to the ganglion cell. At this stage, a number of bipolar cells converge onto the same ganglion cell to produce the larger Y-unit receptive field, as discussed in Section 2.1.3. Finally, we suggest that the non-linearities exhibited by Y-type responses are produced by a rectification in this bipolar-to-ganglion connection. This suggestion is consistent with the conclusion of Hochstein & Shapley [1976b] that Y units are composed of smaller, rectifying, sub-units. As we shall see, this rectification can account for the observed non-linearities in Y-type responses. The rectification in the bipolar-ganglion conncetion has been modeled by assuming that positive signals are essentially unaltered in their transmission from the bipolar to the ganglion cell, while negative potentials are attenuated by a factor of 0.6. (Rectifying synapses of this type are not uncommon. They would correspond to the inward going rectifying membrane in [Jack, Nobel & Tsien, 1975, pp. 225-260].)

In addition to the bipolar cell input, the ganglion cell also receives input from the amacrine cell (shown to be inhibitory in the mudpuppy, [Miller & Dacheux 1976a, b, c]). The amacrine cell's response is discussed in some detail in the subsequent section. For the present, it is sufficient to note that for abruptly changing stimuli the (transient) amacrine response is a brisk on-off response, as illustrated in Figure 5-E. Figure 5 summarizes

the Y-type response to full-field stimulation turning on and off, that results from combining the bipolar and amacrine contributions. The bipolar cell's response (5-A) is transformed by the derivative-like operation (5-C) and rectified (5-D). In the ganglion it is combined with the amacrine's inhibitory contribution (5-E) to produce the final response (5-F). The amacrine cell's input to the ganglion cell is delayed with respect to the bipolar cell input. This delay can be caused, at least in part, by the spike-generating mechanism, i.e, the time required for the charging of the cell's membrane to the spike threshold. The length of the delay depends on the stimulus intensity, and varies between about 20-40 msec. in lower vertebrates. [Werblin & Dowling, 1969; Werblin & Copenhagen 1974; Werblin, 1977, in the mudpuppy; Marchiafava & Torre, 1978, turtle]. It was taken as 30 msec in the model.

The final response is compared (Fig. 5-F, the inset) with a physiological recording from the monkey [De Monasterio, 1978b]. For qualitative comparison, lower vertebrate recordings are shown in 5-a and 5-e. The inset in 5-A is a recording from the goldfish [Kaneko, 1970], and in 5-E the inset shows a recording from the mudpuppy [Miller & Dacheux, 1976a].

Note in conclusion that there are two sources for the additional transience of the Y-response. The first and more important is the derivative-like operation which renders the Y-unit unresponsive to stimuli that do not change with time. Second, the amacrine cell can, under appropriate conditions, cause strong inhibition that further shortens the Y-type response.

2.4 The amacrine cell

Most of the amacrine cells recorded from in lower vertebrates exhibited a transient behavior, responding with short bursts of spikes to both increments and decrements of illuminations within their receptive fields [Werblin & Dowling, 1969; Miller & Dacheux, 1976a; in the mudpuppy; Kaneko, 1970; in the goldfish; Marchiafava & Torre, 1978; in the turtle]. The cells were also characterized by a lack of maintained discharge, and spikes of a relatively small amplitude (20-30 mv) and long duration. In a number of studies, the reponses

of amacrine cells were correlated with their anatomical structure. Transient amacrine cells were found to be of the bi-stratified type [Chan & Naka, 1976; in the catfish, Tachibana, 1980; personal comunication, in the carp]. This stratification enables the cells to collect inputs from depolarizing as well as hyperpolarizing bipolar cells. Since the amacrine cell receives its input from the bipolar cell at the dyad, their input will be, according to the hypothesis of the last section similar to the input to the ganglion cell (see section 4.2). Unlike the ganglion cells, however, the same bi-stratified amacrine cell collects inputs from both hyperpolarizing and depolarizing bipolar cells. If these antagonistic inputs were simultaneous and of equal magnitude, the combined response would have been nullified. There is some evidence, however, that they do not arrive at the amacrine cell simultaneously. There seems to be a delay (10 msec. or more, in lower vertebrates) between the inputs from the depolarizing and the hyperpolarizing bipolar cells [see Marchiafava & Torre, 1978, Fig. 13, in the turtle. In the mudpuppy the depolarizing bipolars are delayed by up to about 90 msec., Nelson, 1973]. Such a delay is a sufficient (although not necessarily the only) cause for the combined response not to be nullified. Furthermore, the amacrine cell would respond to both increments and decrements of light, and the magnitude of the response would depend on the stimulus' rate of change. For an image moving across its receptive field, the response of the amacrine cell will increase therefore with an increase in the stimulus speed. The calculated effect of the speed of movement of a thin bar on the maximal response of the amacrine cell is summerized in Figure 6. The graph shows the maximum in the combined input from hyperpolarizing and depolarizing bipolar cells within a diamater of 100μ, for a delay of 1 msec. of the hyperpolarizing with respect to the depolarizing bipolars. The graph has a sigmoid shape, rising sharply in the 3 – 100 w/sec speed range (where w is the diameter of the receptive field center), and then leveling off. For sufficiently high speeds, the amacrine cell's activity will reach its spiking threshold, causing a sharp decrease in the ganglion activity. This decrease can be observed in Figure 5-F and in Figure 16, computed for a speed of 50 w/sec. For lower speeds, the amacrine cell would not reach threshold, its contribution will therefore be negligible, and the final Y-response would resemble the derivative-like transformation of the X-response without further modifications.

Analogous amacrine responses will be produced by the temporal modulation of standing gratings. When

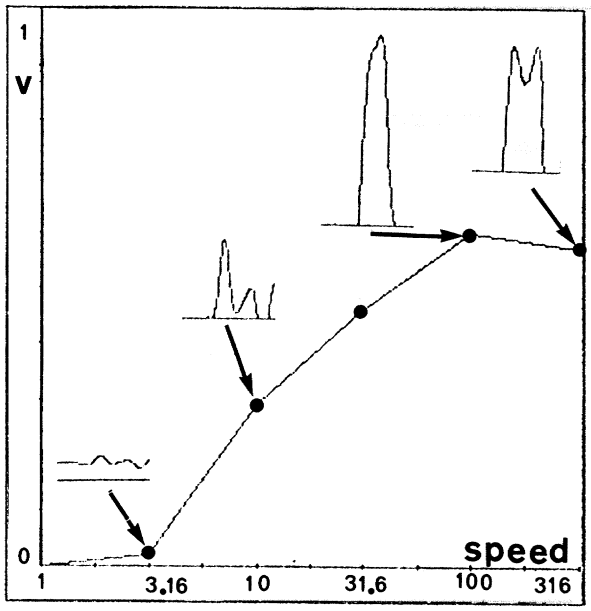

Figure 6. Simulated amacrine cell response as a function of the speed of movement of a thin bar. The amacrine cell recieves opposite input from depolarizing and hyperpolarizing bipolar cells. One input is delayed relative to the other one (see text). The temporal overlap of the two opposing inputs decreases with the speed of movement of the image. Consequently, the greater the speed of movement, the larger the combined response will be. The amplitude of the combined input to the amacrine cell is shown as a function of the speed of movement of a thin bar. The insets are parts of the simulated inputs showing their amplitude. Calibration: Abscissa – speed of movement in w/ sec., Ordinate – relative input amplitude.

the temporal modulation is a square-wave, the amacrine cell's contribution will be significant, while for slow sinusoidal modulation the contribution will be minor. Similarly, when the intensity of a spot of light turning on and off in the center of a Y unit is too low to elicit the amacrine cell's contribution, the Y-response will be prolonged and without the "dip" contributed by the amacrine cell's spiking activity [Cleland &Enroth-Cugell, 1968, fig. 2, De Monasterio 1978b, fig. 2]. In summary, the main effect of the amacrine contribution in our model is in causing the "dip" and further shortening the ganglion cell's response, provided that the stimulus' rate of change is sufficiently high.

2.5 X-type response

X-type response is similar to the response in our model of the bipolar cell [see Naka, 1972, Fig. 5]. Such a similarity may be obtained if the bipolar–to–amacrine transmission in the dyad, or the recurrent synapse of the amacrine onto the bipolar, are relatively ineffective in X-type units, in which case the bipolar signal will be little affected on its way to the ganglion. Note also that in this model amacrine input is not required for the organization of the midget X–units, since their spatial organization occurs at the OPL level.

We have modeled the pure X-response by assuming the extreme case of a completely ineffective transmission in the bipolar–amacrine connection, obtaining an X-response that is essentially equivalent to the bipolar response described in Sections 2.1–2.2. Intermediate units with a combination of X and Y temporal properties can in principle be obtained by a gradual increase in the efficiency of the dyad's derivative-like operation. This mechanism could also serve as the contrast– gain–control if the synaptic efficiency is gain controled [shapely et. al. 1978]. Recent results by Shapely & Victor [in preparation] support the existence of a feedback mechanismwhich is (i) more effective in Y then in X units, and (ii) controlled by contrast. The transience and the nonlinearity characteristics of the cells' behavior are not necessarily tightly linked, since the first is generated in the bipolar–amacrine interconnections while the second is introduced in the bipolar to ganglion transmission.

3. Simulation Results

In this part, the simulated X- and Y-responses to a variety of stimuli will be described and compared with electrophysiological recordings whenever available.

Before describing the results, we shall summarize the parameters and assumptions incorporated in the model, and the method of computing the X- and Y-response to an arbitrary spatio-temporal pattern P(x,y,t).

3.1 Summary of parameters and assumption

The bipolar response BP(t) in computed in the model by:

$$BP(t) = C(t) - S(t - \delta t)$$

where C(t) is the center response, S(t) the surround response, and δt the surround-center delay, taken as 3 msec.

The center response C(t) is obtained by weighing the spatio-temporal pattern P(x,y,t) by G_c, the central gaussian of the receptive field, and convolving the result with $I_c(t)$, the temporal impulse response function of the center mechanism. In mathematical notation:

$$C(t) = I_c * \int G_c(x, y) \cdot P(x, y, t) dx dy$$

Similarly, the surround response S(t) is given by:

$$S(t) = I_s * \int G_s(x, y) \cdot P(x, y, t) dx dy$$

where G_s is the gaussian shape of the surround mechanism, and I_s the temporal impulse response of the surround mechanism.

For the midget bipolar receptive field, G_c and G_s can be approximated by two-dimensional gaussians with space constants of 25" and 50" of arc respectively. For the flat bipolar the space constants are 35" and 75" of arc for the center and surround mechanisms respectively.

The temporal impulse response functions I_c and I_s were both modeled by the impulse response of an RC circuit, i.e., $\frac{1}{\tau} \cdot e^{\frac{-t}{\tau}}$. The time constant τ was taken as 10 msec. for the center response and 20 msec. for the surround.

A Pure X-type response is identical in the model to the computed bipolar response, in the sense that the changes in its rate of discharge follow the changes in the bipolar cell's membrane potential. Since X units may differ in size (depending, e.g., on retinal eccentricity), we expressed the dimensions of the stimuli in terms of w, the diameter of the receptive field center. For example, the speed of moving stimuli was expressed in units of w/sec.

A Y-type response is computed by integrating the contributions from all the (flat) bipolars within a radius of 100μ, and assuming that the density of flat bipolars of a given polarity in the fovea is about half the cone's density (as suggested, e.g., by the data in [Kolb, 1970]. Each flat bipolar contacts 5–7 cones, and each cone is contacted by up to six flat bipolars. The ratio between cones and flat bipolars of both polarities is therefore about 1). The contribution of each bipolar cell to the Y-response is obtained by passing the bipolar signal BP(t) through the derivative-like operation shown in Figure 5-C. This function was generated by simulating two reciprocal synapses, as explained in the discussion.

The response is then rectified: the positive part is unaltered, while the negative part is multiplied by 0.6. The Y-unit then integrates the responses using a the weighting function described in section 2.1.3. The Y-response can be summarized as:

$$Y(t) = \sum_i [w_i \cdot (BP_i * d(t)] - Amacrine$$

where i ranges over all the bipolars that contribute to the unit's response, and w_i the weight of the i^{th} unit.

The amacrine cell's response was computed by integrating all of the depolarizing as well as hyperpolarizing bipolar cells within a radius of 100μ, with the contribution of the hyperpolarizing bipolars delayed by 1 msec. (The net input to the amacrine cell dependes only on the delay between the two bipolars and not on the order of their inputs.) We did not have to set a precise threshold for the amacrine cell. The simulations fell

naturally into two classes: for sinusoidal modulation and slowly drifting stimuli (about 3 w/sec) the amacrine input is small, and it can be assumed that it did not reach its threshold. For square-wave temporal modulations and fast moving stimuli the input to the amacrine was large: it can be seen (Fig. 6) that increasing the speed to 50 w/sec increases the input to the amacrine almsot a hundred fold. For these conditions it can therefore be assumed that spiking threshold has been reached, and the spike train was therefore superimposed on top of the slow potential component, e.g. fig. 5–E.

3.2 Flickering spot of light

3.2.1. X-type response

In this section we shall examine the simulated X-type response to a spot of light turning on and off in three positions in the receptive field: center (Fig. 7A), surround (7C), and the center-surround boundary (7B). The simulated results are compared with physiological recordings from the monkey (taken from De Monasterio, 1978b) and the cat (from Ikeda & Wright, 1972).

Flickering dot at the center of the receptive field

The simulated X-type response (of an on-center unit) to a flickering spot of light at the center of the receptive field is shown in Figure 7A-1, and compared with physiological recordings from the monkey (A-2) and cat (inset). The response is computed in the model from the difference between the center and surround responses. For an increment in light the combined response is given by:

$$C \cdot (1 - e^{\frac{-t}{10}}) - S \cdot (1 - e^{\frac{-(t-3)}{20}})$$

where C and S are the relative strengths of the center and surround contributions.

Spatially, the X-unit's receptive field has the shape of a balanced difference-of-gaussians. In such a shape the ratio between the peak responses of the center and surround mechanisms is the inverse of the ratio between their respective space constants. For X-units this ratio is approximately 1.5-2.0 (Rodeick, 1965b; Bullier & Norton, 1979; Figure 2). At the center-surround boundary C = S, and in the receptive field's periphery C

$\ll$ S. We conclude that even an ideal X-type response can exhibit a marked transient component, but that its steady-state response for a light spot in the center should exceed half its peak value.

Flickering dot in the periphery of the receptive field

When the flickering dot is positioned far enough in the periphery of the receptive field, the overall response will be dominated by the surround contribution. The response will then have the shape of the voltage change across a charging or discharging capacitor. The time course will be slower than the response to a dot at the center. This response is simulated in Figure 7C-1, and compared with a recording from the monkey (C-2) and cat (inset).

Flickering dot at the center–surround boundary

At the center-surround boundary the center and surround responses are of equal amplitudes and opposite signs. The overall response will therefore be small and entirely transient (i.e., no steady state response). The simulated response at this position is shown in Fig. 7B, together with a corresponding recording from the cat (inset).

The responses of off-center units will be similar to those of the on-center one, but of the opposite polarity. For example, it will be deeply inhibited by the onset of a dot at the center, and will have a positive response when the dot is turned off.

3.2.2 Y-type response to a flickering dot

Flickering dot at the receptive field center

The simulated Y-type response to a small spot of light turning on and off at the center of the receptive field of an on-center unit is illustrated in Figure 8A-1, and compared with corresponding recordings from the monkey (A-2, from De Monasterio 1978b) and the cat (A-3, from Cleland & Enroth-Cugell, 1968. The cat's unit was not classified originally as a Y cell, but was classified so by us according to its response). The response

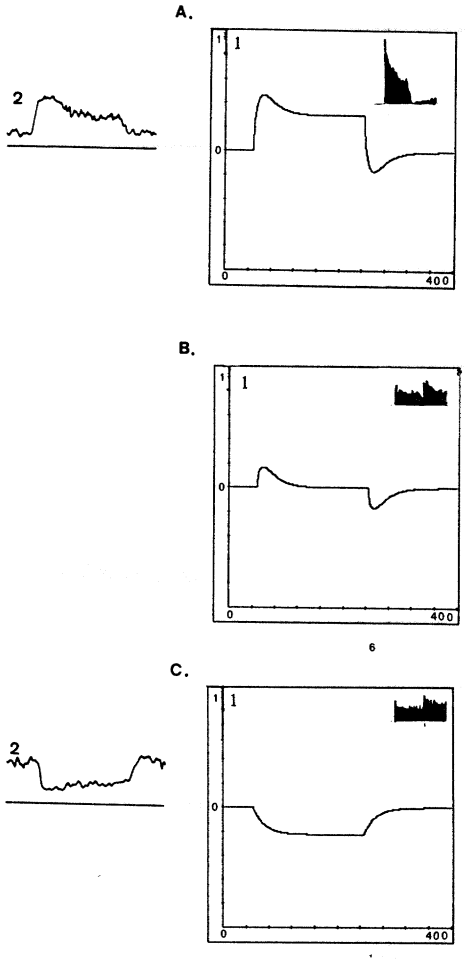

Figure 7. Response of an on-center X-ganglion cell to a spot of light at different positions in the receptive field. A-1: the response to a spot located at the center of the field. A-2 is a corresponding recording from a monkey [De Monasterio 1978 a, fig. 5] B-1: the response to a spot located at the center - surround boundary. C-1: the response to a spot located at the periphery. C-2: the corresponding recording from a monkey [De Monasterio 1978 a, fig. 5]. The insets in A-1, B-1 and C-1 are corresponding recordings from a cat [Ikeda & Wright 1972, fig 1]. Calibration : Abscissa – time in milliseconds, Ordinate – relative response.

is entirely transient – it has no steady state component. The "on-dip" (that is, the sharp decrease following the initial rising phase) is contributed in the model by the amacrine cell. The on-dip was described originally by Saito, Shimahara & Fukada, [1971] in the cat. De Monasterio [1978b] has demonstrated that its occurence coincides with the proximal negative response of the ERG, attributed to amacrine cells activity.

The amacrine cell's activity has an additional effect: it shortens considerably the overall duration of the response. For similar responses, including the "on-dip" see also [Sherman, Wilson, Kaas & Webb, 1976; Schiller & Malpeli, 1977; Bullier & Norton, 1979b].

Flickering dot at the center-surround boundary

At the center-surround boundary, the Y-unit will respond to the onset as well as the termination of the stimulus (Fig. 8B-1). This "on-off" response is characteristic of Y-type units, and therefore we have classified the recordings in 8B-2 (from Rodieck & Stone, 1965a; in the cat) and the discharge pattern in the inset (from Kuffler, 1953; in the cat) as Y-type responses (both of these recordings predated the original X/Y classification). The main cause for the additional off-response, according to the model, is the derivative-like operation in the IPL. The model predicts, therefore, that units classified as Y-type on the basis of transient response to a spot in their center, would also exhibit the on-off response at the center-surround boundary. The model predicts that at the exact center-surround boundary there will only be a weak off-response. To get on- and off-responses of roughly equal amplitudes, the dot has to be displaced towards the surround region of the receptive field. (The underlying reason is the difference in the time constants of the center and surround mechanisms.)

Flickering dot in the surround

As the flickering spot of light is moved further towards the periphery of the Y-unit's receptive field, the on-response diminishes in amplitude and the off-response increases. A simulated surround response is illustrated in Fig. 8C-1. According to the model, a short inhibitory period separates the off-response from the termination of the stimulus. An exclusive off-response with an apparent delay can be seen in the discharge pattern in the inset (from Kuffler, 1953, same unit as in A-1 and B-1). Again, we did not have a comparable

response from a unit already classified as Y-type, but we can predict that the off-response and its delay would be characteristic of Y-units. The simulated Y-responses to flickering dots are also in good agreement with the spatio-temporal diagram in Bullier & Norton [1979b, figs. 1,4). Although the diagram was plotted using a flickering bar rather than a dot, the results are qualitatively comparable, owing to the circular symmetry of the receptive field.

The Y-response simulations were all for on-center units. An off-center unit would have similar responses, but of the opposite polarity. It will have an off response in the center, on response in the surround, and on-off response at the center-surround boundary. The on response will be preceded by a short inhibitory period.

3.3 Full-field stimulation

In this section we shall compare the simulated and empirical responses to an increase and decrease in illumination across the entire receptive fields of X- and Y-units.

3.3.1 X-type response to full-field stimulation

Since the modeled receptive field of X-units has the shape of a balanced difference-of-gaussians, it will have no steady-state response to full-field stimulation. It will exhibit, however, a short transient response when the illumination is increased or decreased. For on-center units, the response will be positive for increment and negative for decrement in the overall illumination. This transient response in pure X-units is caused by the delay between the center and surround mechanisms in the OPL.

The X-type simulated response to full-field simulation is shown in Figure 9C-1, and compared with recordings under similar conditions from the monkey (C-2, from De Monasterio, 1978b) and the cat (C-3, from Enroth-Cugell & Robson, 1966). The unit's response is qualitatively similar to its response to a spot of light flickering at the center-surround boundary (compare with Fig. 7B). The stimulus employed in the recordings extended over most, but not necessarily all of the receptive field. This may account for the residual steady-state response in them. The simulated response is entirely transient. If, however, the unit is not balanced (center stronger then surround), then a sustained component would be observed.

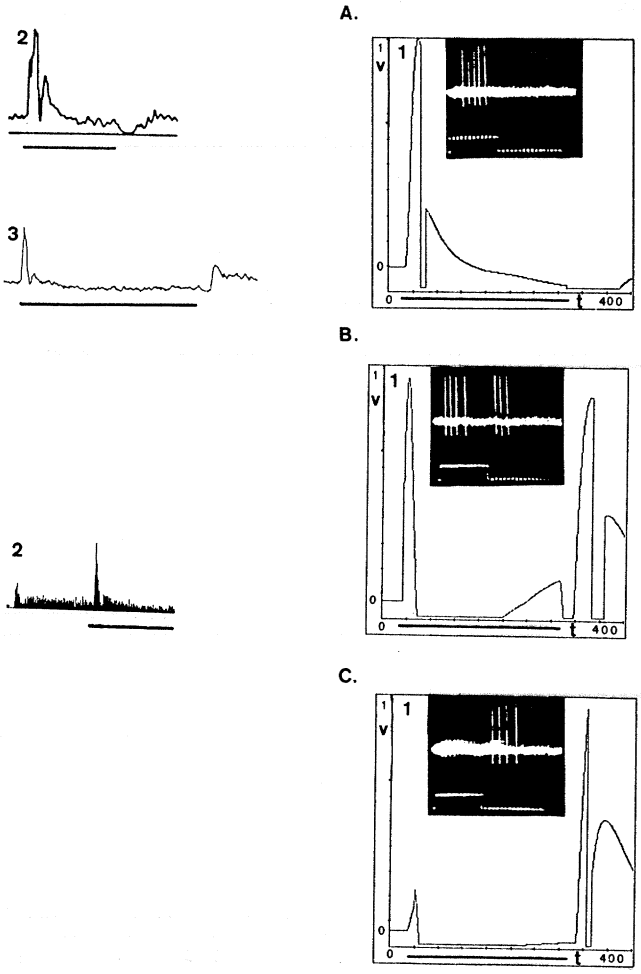

Figure 8. Response of an on-center Y-ganglion cell to a spot of light at different positions in the receptive field. A-1: the simulated response of the cell to a spot at the center of the field. A-2 and A-3 are the corresponding recordings from a monkey [De Monasterio 1978 b, fig. 2] and a cat [Cleland & Enroth - Cugell 1968, fig 2] respectively. Note the dip following the initial increase in the rate of dischage (A-2, A-3) and the corresponding one in the model (A-1). B-1: the simulated response to a spot at the center surround - boundary. B-2: a corresponding recording from a cat [Rodieck & Stone 1965 a, fig 5]. Note the on - off response. C-1: the simulated response to a spot at the periphery . The insets in A-1, B-1 and C-1 are spike discharges in corresponding conditions in a cat [Kufller 1953]. Calibration : Abscissa – time in milliseconds, Ordinate – relative response.

3.3.2 Y-type response to full-field stimulation

The simulated Y-response to full-field stimulation is shown in Figure 10C-1, and compared with recordings made under similar conditions in the monkey (C-2, De Monasterio 1978a) and the cat (c - 3, Enroth-Cugell & Robson, 1966). As for the X-units, the recordings were made with stimuli extending over most of the receptive field, but not covering it completely. The response is qualitatively similar to the Y-type response to a flickering dot in the central region of the receptive field. Both have strong on- but little or no off-response (compare with Fig. 7A).

A general observation from the above simulation is that the sustained / transient dichotomy requires some caution. Although the X-type response is on the whole more sustained than the Y-type, the nature of the temporal response depends also on the stimulus and its position. Even an ideal X-type response will exhibit a transient component to a flickering dot in the unit's center. For a point at the center-surround boundary, or for full-field stimulation, the response will be entirely transient (c.f. Kuffler, 1953; De Monasterio, 1978a).

3.4 Alternating edge

The stimulus in this condition is a single intensity edge positioned within the unit's receptive field. The edge is modulated as a function of time – the two half-fields alternate in counterphase. In this section the X- and Y-type responses to an alternating edge at various positions within the receptive field will be examined. This stimulus (and the alternating gratings considered in the subsequent section) are of interest since they are commonly used to classify X and Y responses. X-units are linear, hence they will have no response to an edge passing through the middle of the receptive field. Y-units, in contrast, have no such null position.

3.4.1 X-type response to an alternating edge

The X-type responses to an alternating edge at different positions within the unit's receptive field are shown in Figure 9. When the edge passes through the center of the receptive field, the simulated response is zero (9A-1). This null position is shown in the recordings in 9A-2 (De Monasterio, 1978b; from the monkey), and 9A-3 (Enroth-Cugell & Robson, 1966; from the cat, using a 0.16 c/deg. square wave grating).

When the edge is displaced towards the periphery of the receptive field, positive and negative responses to the opposite phases of the alternating edge begin to emerge (9B-1, where the edge was displaced by 0.5 w). Figure 9B-2 illustrates a similar recording from the monkey (by De Monasterio, 1978b). The position of the edge is illustrated in the inset. As the edge is displaced further towards the periphery of the receptive field, the responses (both positive and negative) gradually increase. Finally, when the edge is far enough in the periphery, the situation is essentially the same as the full-field condition examined in the preceding section (Fig. 9C).

3.4.2 Y-type response to an alternating edge

When the alternating edge passes through the middle of a Y-unit, the response will not be nullified. The main reason (in the model) is in the rectification effect. Being rectified, the negative contributions no longer cancel out the positive ones. The response will therefore exhibit frequency doubling: it will respond twice within each cycle of the alternating edge. The main contribution to the response comes from the half-field that is turning on (for an on-center unit). In this sense it is an "on-on" response, in contrast with the "on-off" response to a flickering dot (Fig. 8B). While the frequency doubling in the on-on response is causes primarily by the rectification, the on-off response is causes primarily by the derivative-like operation. Cells with marked transience but little or no non-linearity are therefore expected to exhibit a frequency doubling to a flickering dot (positioned appropriately), but not to an alternating edge.

The simulated response in 10A-1 is compared with recordings from the monkey (A-2, De Monasterio 1978b), and the cat (A-3, Enroth-Cugell & Robson, 1966).

As the edge is displaced towards the periphery of the receptive field, one side of the edge (the "major" side) will cover a larger portion of the receptive field's area. The unit will now respond more strongly to the on phase of the major side than to its off phase. Finally, when the major side covers the entire receptive field, the situation becomes identical to the full-field condition examined in the pervious section, and the off response will become greatly reduced or absent. The full-field condition in Fig. 10C was considered in the preceding

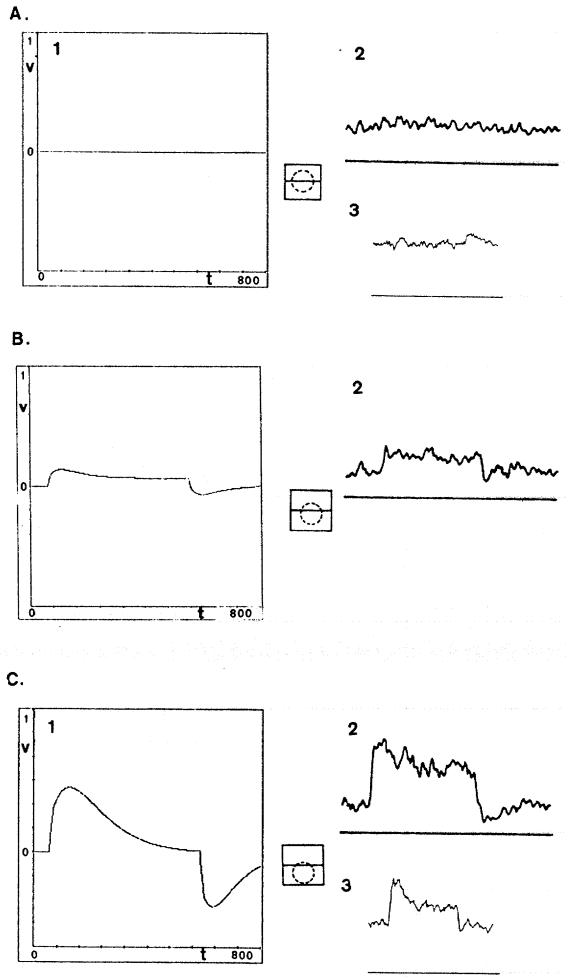

Figure 9. Response of an on-center X-ganglion cell to an alternating edge at different positions in the receptive field. The edge is alternating in time (square wave modulation). The position of the edge relative to the receptive field is indicated in the middle column. A-1, B-1 and C-1 are the responses to 0.5 Hz. stimulaton. A-2, B-2 and C-2 are the corresponding recordings from a monkey [De Monasterio 1978 b. his square wave modulated bipartite field]. A-3 and C-3 are corresponding recordings from a cat [Enroth - Cugell & Robson 1966, their low spacial frequency square wave modulated stimulus, fig. 1]. Note the null point at the center of the receptive field (A). The responses in C-2 and C-3 are not entirely transient, probably because the field was not completly covered. Calibration : Abscissa – time in milliseconds, Ordinate – relative response.

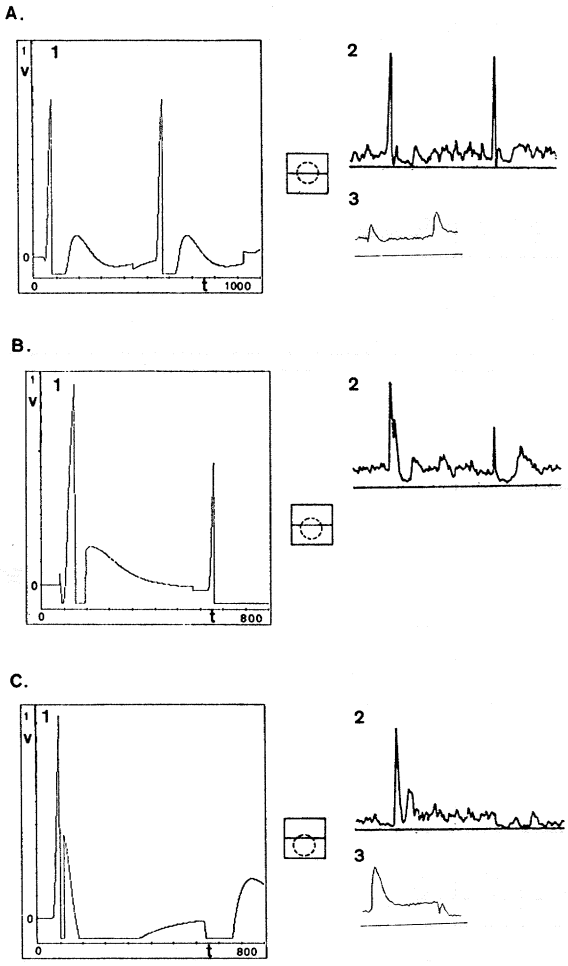

Figure 10. Response of an on-center Y-ganglion cell to an alternating edge at different positions in the receptive field. All the graphs are for the same stimulation conditions as in figure 9. Note the frequency doubling at the position where the X-cell had a null point (figure 9). The physiological recordings are from a monkey [De Monasterio 1978 b, A-2, B-2 and C-2] and from a cat [Enroth - Cugell & Robson 1966, fig. 1,A-3 and C-3].

section. An intermediate position of the edge is shown in Fig. 10B-1 and compared with a recording from the monkey (B-2, De Monasterio, 1978b). Additional recordings of Y-unit responses to an alternating edge at various positions in its receptive field are found in Bullier & Norton 1979a, Figure 12.

Similar results are obtained when the edge is modulated sinusoidally in time (rather than alternating). Frequency doubling would occur when the edge is positioned in the middle of the receptive field, but not when it is displaced sufficiently towards the unit's periphery. Figure 11 illustrates the simulated Y-response to a sinusoidally modulated edge at two positions in the receptive fields (shown in the insets, lower row). These responses are compared with recordings from the monkey (by De Monasterio, 1978b). The main distinction between sinusoidal and square-wave modulations is the lack of the on-dip in the former. The on-dip is attributed in the model to the amacrine cells' spiking activity. This activity is low for gradual temporal changes, consequently the absence of the on-dip for sinusoidal modulation is not unexpected.

3.5 Alternating gratings

The stimuli considered in this section consist of a grating with a sinusoidal spatial modulation and a square-wave temporal modulation. We shall examine the response of X and Y units, and the effect on their response of the gratings' position and spatial frequency.

3.5.1 X-type response to alternating gratings

Qualitatively, the X-type response to alternating gratings is similar (both in the model and in the empirical data) to its response to an alternating edge. The response will have a null position when the gratings are positioned anti-symmetrically with repect to the unit's center. The modeled response to gratings has a band-pass shape as a function of spatial frequency (i.e., strong attenuation for both high and low spatial frequency). The exact shape of the response curve as a function of temporal modulation frequency depends on the particular stimulus used. Qualitatively, it has the shape of a low-pass filter with peak reponse in the region of about 6-8 Hz [c.f. van de Grind, Grusser & Lunkenheimer, 1973] see also fig. 16-a.

3.5.2 Y-type response to alternating gratings

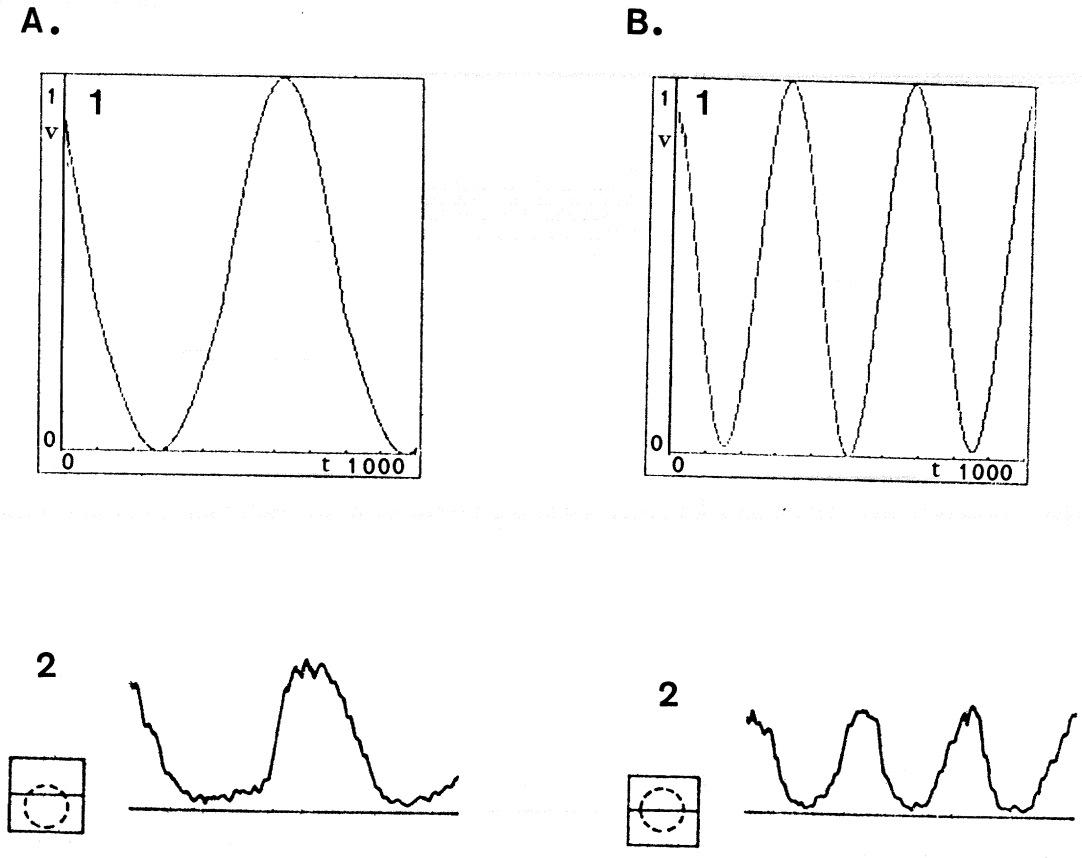

Figure 11. Response of an on-center Y-ganglion cell to a sinusoidally modulated edge. The position of the edge relative to the receptive field is indicated by the insets in A-2 and B-2. For an edge located in the periphery, the response of the model (A-1), as well as the physiological recording from a monkey (A-2), were modulated sinusoidally with a frequency equal to that of the stimulus. For an edge located in the center of the receptive field, the frequency of the response is doubled (B-1 and B-2). The physiological recordings are from [De Monasterio 1978 b, fig. 7]. Calibration : Abscissa – time in milliseconds, Ordinate – relative response.

For sufficiently high spatial frequency, the simulated Y-response exhibits a frequency doubling irrespective of the stimulus position within the receptive field. The main reason is that, as a resut of the rectification, the negative contributions are insufficient to nullify the positive ones. The simulated response for high spatial frequency (1.0 cycle/w), is shown in Figure 12A-1 and A-2 for two different positions within the receptive field. A change of 1/4 cycle in the position of the grating (90 deg in spatial phase) has only a minor effect on the response. The simulated response is compared with physiological recordings from the cat in Figures 12A-3,4, and 5, where the frequency doubling and the lack of dependence on position can be observed.

At low spatial frequency, the simulated Y-response resembles the response to an alternating edge. Gratings placed anti-symmetrically with respect to the unit's center give rise to on- and off-responses of similar size (Fig. 12B-1, the spatial frequency is 0.5 cycle/w.). When the gratings are placed symmetrically with respect to the unit's center, the off-response diminishes in size relative to the on-response (12B-2). Similar responses were obtained in the cat by Enroth-Cugell & Robson [1966] (12B-3 and B-4), and by Hochstein and Shapely [1976a] (12B-5 and B-6).

Pure Y-units in the model exhibit a band-pass response as a function of spatial as well as temporal modulation. The simulation curves are in general agreement with the experimental data [c.f. van de Grind, Grusser & Lunkenheimer, 1973] see also fig. 16-b.

3.6 Moving stimuli

In this section, the X- and Y-type responses to edges, bars of different widths, and gratings, moving at different speeds, will be examined.

3.6.1 X-type response to moving stimuli

To a first approximaion, X-type response to a moving stimulus can be obtained by a convolution of the DOG-shaped receptive field (scaled in proportion to the velocity) with the stimulus. This procedure was used by Marr & Ullman [1979], and their results for an edge, thin bar (bar width = 0.5w, where w is the diameter of the receptive field center), and wide bar (bar width = 2.5w), are shown in Figure 13-C. The predicted

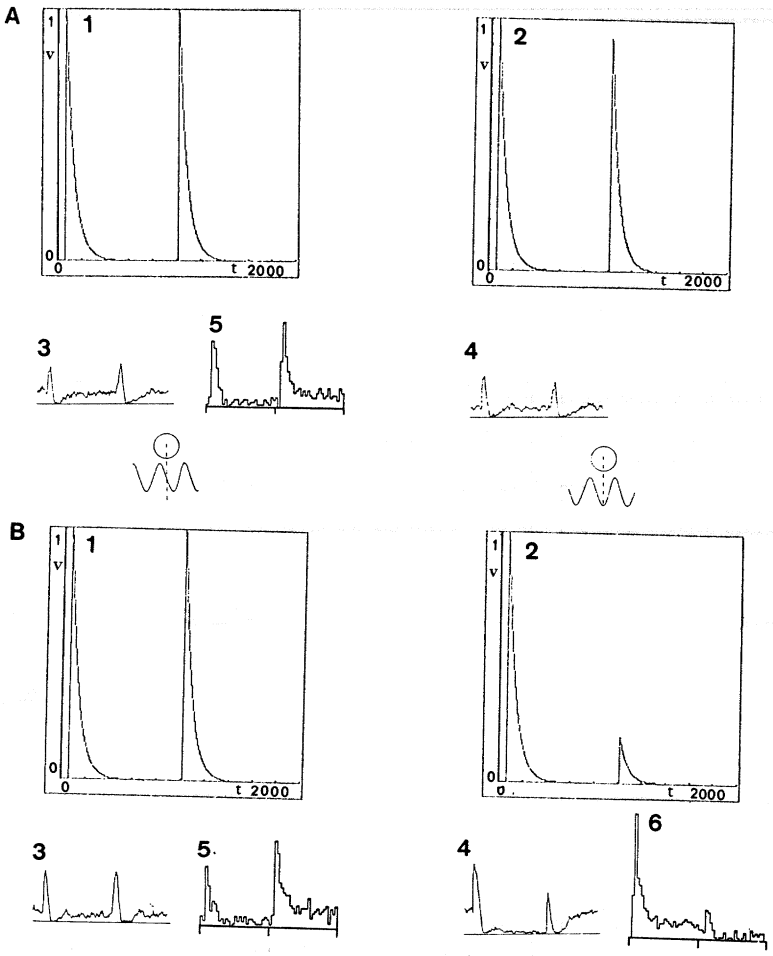

Figure 12. The effect of spatial frerquency and phase on Y-cell's response to alternating gratings. The stimulus was an alternating (square wave modulated in time) sinusoidal grating. The spatial phase of the grating was varied, as indicated by the place of the sine-wave relative to the circle (representing the receptive field). At a high spatial frequency (1.0 c/w) a 90 deg. change in the spatial phase caused a little change in the reponse and the response frequency was twice that of the stimulus (A-1 compared to A-2). A-3 and A-4 are from a cat, using spatial frequency of 0.64 c/deg. [Enroth - Cugell & Robson 1966, fig. 3]; A-5 is from a cat, using spatial frequency of 0.7 c/deg. [Hochstein & Shapley 1976 b, fig. 5]. At a low spatial frequency (0.5 c/w) one spatial phase gave rise to frequency doubling (B-1), whereas at 90 deg. phase shift one of the responses was drastically reduced (B-2). B-3 and B-4 are from [Enroth-Cugell & Robson 1966, fig. 3] using spatial frequency of 0.16 c/deg.,and B-5 and B-6 are from [Hochstein &Shapley 1976 b, fig. 5] using spatial frequency of 0.35 c/deg. The Amacrine cell's inhibition was not included in this case, it may add an on-dip and truncate the response. Calibration: Abscissa – time in milliseconds, Ordinate – relative response.

response of the model for the same stimuli (moving at 3 w/sec) is illustrated in Fig. 13-B. The deviations of the model from the calculated responses in 13-C are caused primarily by the delay between the center and surround mechanisms. The effect of this delay can be visualized as a convolution of the signal with a DOG-shape in which the positive and negative gaussians no longer coincide. The negative gaussian "lags behind" by a distance of $v \cdot \tau$, where v is the stimulus' speed and τ the surround-center delay, as illustrated in Fig. 14. The assymetries introduced to the modeled response in this way can also be observed in the physiological recordings (13-A). The recordings in 13-A are shown in a format called "response curves" by Rodieck [1965]. Each response is a composite of a positive and a negative part, taken from on-center cells stimulated with opposite contrasts. The edge traces are from Dreher & Sanderson [1973, Fig. 6 d & e], and the bar traces are from Rodieck & Stone [1965, Figs. 1 & 2, using bars 1 and 5 degrees wide]. The edge traces were recorded in the LGN. They can nevertheless be used for comparison since retinal and LGN units were found to match closely in their reponses [Cleland, Dubin & Levick 1971; Sherman *et al.* , 1975; Bullier & Norton, 1979a,b].

3.6.2 Y-type responses to moving stimuli

The predicted Y-type responses to an edge, a thin bar, and a wide bar moving at a speed of 3 w/sec are shown in Figure 15-B. The curves in 15-C are the responses calculated in Marr & Ullman [1979] by taking the temporal derivative of their calculated X-type response. It can be seen that the two are in good overall agreement, supporting the derivative-like operation hypothesis (Section 2.3). The deviations are caused by a combination of three factors: (i) the surround-center delay, (ii) the deviation of the derivative-like operation from an exact mathematical derivative, and (iii) the rectification. The deviations will become more pronounced at higher speeds where, in addition, the amacrine cell's contribution will also become noticeable.

The simulated responses are compared in Fig. 15-A with electrophysiological recordings, presented in the same form as in Fig. 13-A. The traces are taken from Dreher & Sanderson [1973, Figs. 6b, 8a, for edge responses; 1d, 2c for the thin bar; 2b for off-center response to a wide bar], and from Rodieck & Stone [1965; Fig. 5b for on-center response to a wide bar]. The units in these recordings where not identified originally as Y-units. We have classified them as Y-type responses based on their close agreement with the expected Y-

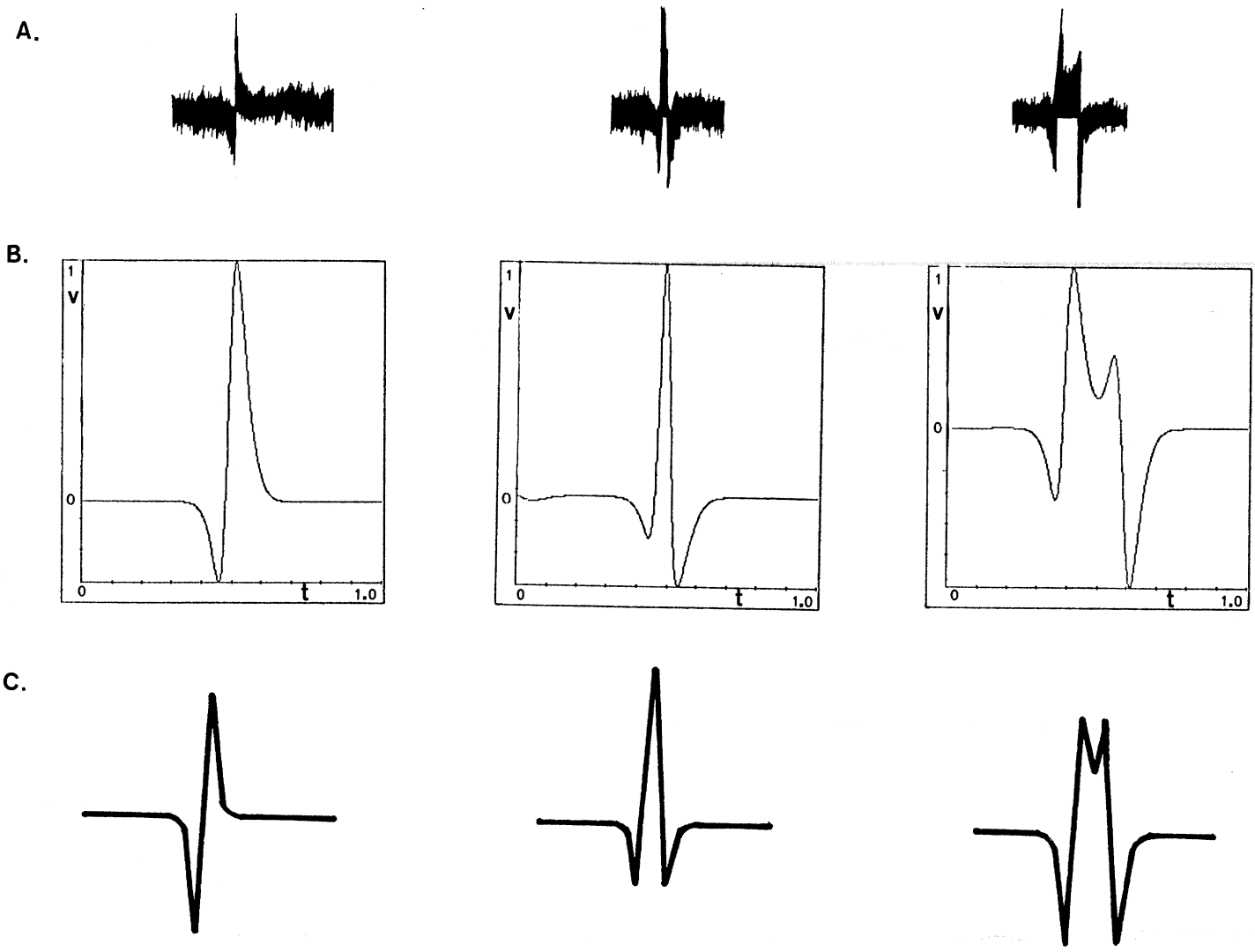

Figure 13. Response of an X-ganglion cell to moving stimuli. The columns from left to right are for a moving edge, a moving thin bar and a moving wide bar. A: response curves, prepared in the format used by Rodieck (1965). The positive and negative parts of the composite response are from recordings with opposite contrasts. The recordings are from Dreher & Sanderson (1973, fig 6-b) for the edge and from Rodieck & Stone (1965 b, fig. 1 and 2) for the bars. B: the predictions of the model. C: the theoretical responses used by the computational model of Marr & Ullman (1979). The asymmetries in the model are caused by the delay between the surround and the center mechanisms (see figure 14). Calibration : Abscissa – time in seconds, Ordinate – relative response.

responses, but not the X-responses (as can be seen from a comparison of Figures 13, 15).

3.6.3 Responses to moving gratings

For slowly moving gratings (modulated sinusoidally in space), the X-type response will have a sinusoidal shape with the same frequency and about the same phase as the input. As the speed of the gratings is increased, the surround-center delay will introduce some distortions in shape, a gradual phase shift, and (for sufficiently high speeds) a decrease in amplitude. The response is maximal, in the model, for motion that produces a temporal frequency of 6-8 Hz. Such responses are reported by De Monasterio [a] in the monkey.

Y-type response to slowly moving gratings is roughly a temporal derivative-like transformation of the input. The predicted response is therefore shifted by about 90 deg in phase with respect to the input. Such a phase shift can be observed in the recordings of Schiller & Malpeli [1977, Fig. 9a, color-opponent *vs.* broad-band], and of De Monasterio [1978a, Figs. 8a & 9a]. The dependence of the response on the spatial frequency of the moving gratings is shown in figure 16-a for X-type and 16-b for Y-type. The "X"s are the simulation results and the full circles are experimental data from the cat [Enroth Cugell & Robson, 1966]. The sensitivity is measured as the reciprocal of the contrast at threshold. The temporal frequency for both the simulated and experimental results is 4_{Hz}. Note that although the underlying receptive fields are ballanced (and therefore should have a band-pass fourier transform)their MTF curves have appreciable component at low frequency, due to their temporal characteristics. A secondary effect in the response of Y–cells is the " on – dip" for sufficiently high speeds. At low speed the on – dip is absent (see, e.g., De Monasterio 1978 a, figs, 8-a, 9-a, in a speed of about 7 w/sec.

When the speed of movement is increased to about 50 w/sec [*ibid* , Fig. 9-c] (spatial freq 0.5 w = 0.2, temporal freq = 10) or higher [Fig. 9-d], the on-dip becomes apparent.

Figure 17-A illustrates the simulated Y-response to sinusoidal gratings moving at 50 w/sec. The simulation is compared in Fig. 17-B with De Monasterio's [1978a, Fig. 9-c] recording.

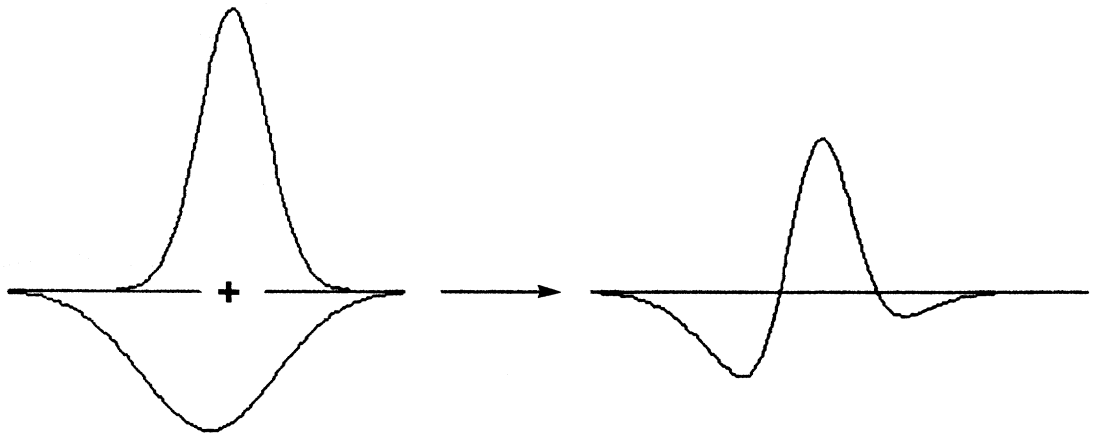

Figure 14. The effective distortion of the receptive field due to motion. Since the surround response is delayed with respect to the center's, for an image in motion across the receptive field, the surround gaussian will effectively trail behind by a distance of $v \cdot \tau$, (where v is the speed and τ the surround-center delay). In this figure the distance between the peaks of the center and the surround gaussians is 0.1 w due to a delay of 3 msec. and a speed of 30 w/sec. (at the left). The resulting distorted field is shown at the right.

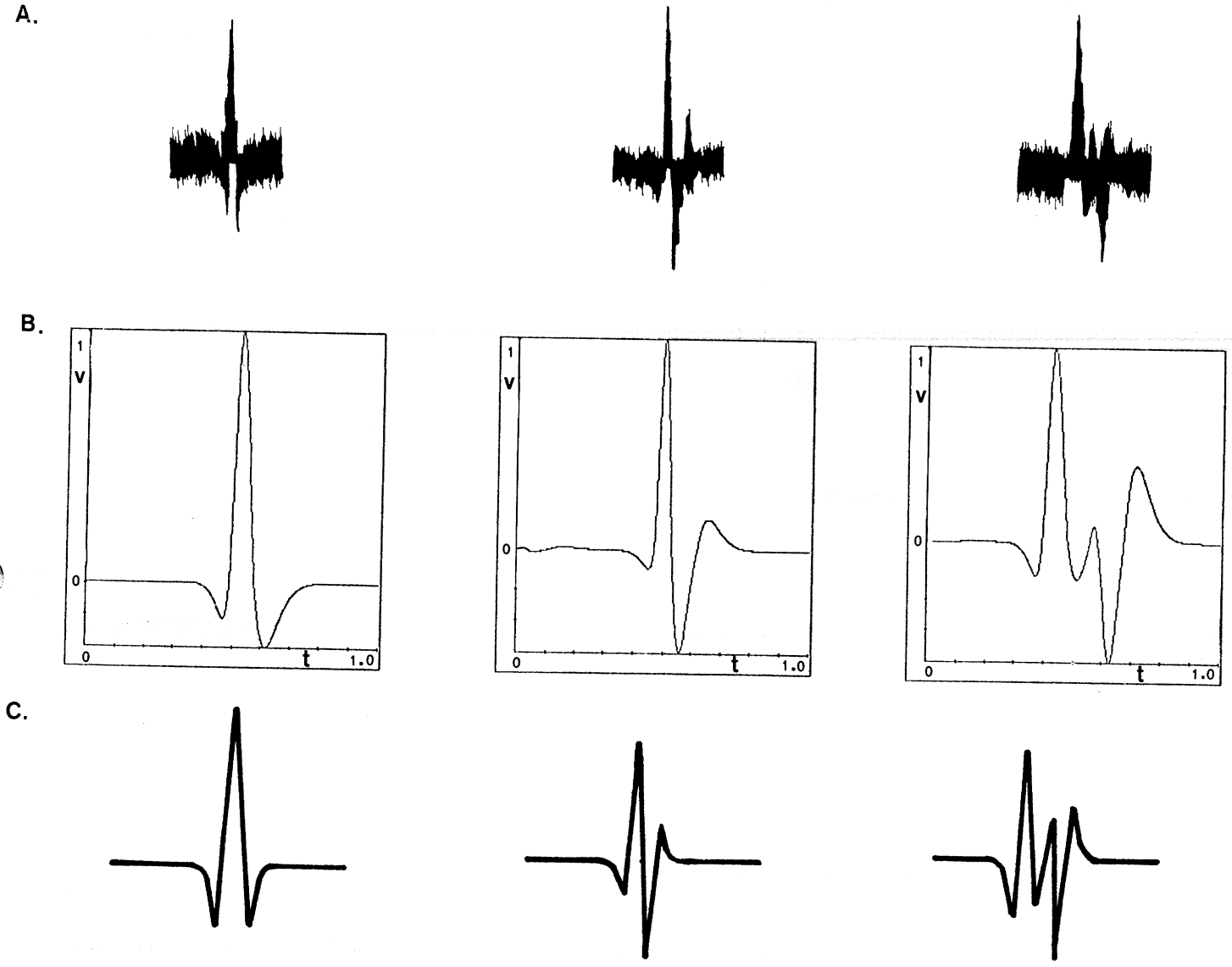

Figure 15. Response of an on-center Y-ganglion cell to moving images. Same stimuli as in figure 10, but for a Y-cell. The response curves are prepared as in figure 13, from Dreher & Sanderson (1973, figs. 1,2 and 6-c) Note that in spite of the delays included in the model, the deviation from a strict temporal derivative and the rectification, the overall derivative-like nature of the response postulated by Marr & Ullman's theory (1979) is well preserved.

4. Discussion

4.1 Summary of interconnections and responses

A schematic diagram summarizing the retinal interconnections and responses that generate, according to the model, the Y-type response, is shown in Figure 17. The curves inside the cell somata show the responses of the cells to a spot of light turning on and off.

4.2 Temporal differentiation in the dyad

The derivative-like operation in the IPL was modeled by computing the affect of the recurrent synaptic arrangement between the bipolar and the amacrine cells, the bipolar-to-ganglion synapse, and the bipolar cable properties. The main conclusion from this computation is that a derivative-like operation can be produced by the synaptic arrangement of the IPL. The input to the dyad, coming from the bipolar cell's soma, is transmitted to the amacrine cell through an excitatory synapse. The potential change that develops in the amacrine cell's process is transmitted back to the bipolar cell through an inhibitory synapse, delayed by the synaptic responses. The recurrent synapse can give rise to a derivative-like operation, as can be seen from the following qualitative argument. A stimulus V(t) arriving to the dyad at time t, is subtracted from the potential in the dyad after a time interval δt — the synaptic delay of the two synapses. This causes the potential at the dyad to change roughly as $V_t - V_{(t-\delta t)}$.

The full calculation of the dyad's response was performed as follows: The input to the bipolar cell was convolved with the cable properties of the bipolar cell [Jack et. al. 1975, p. 52], yielding the input to the dyad, S(t).

$$S(t) = input(t) * t^n \cdot e^{-\alpha t}$$

For the synaptic impulse response, the alpha function [Jack et. al. 1975] was used. The impulse response of the excitatory synapse was thus taken as:

$$EX(t) = E\alpha^2 \cdot te^{-\alpha t}$$

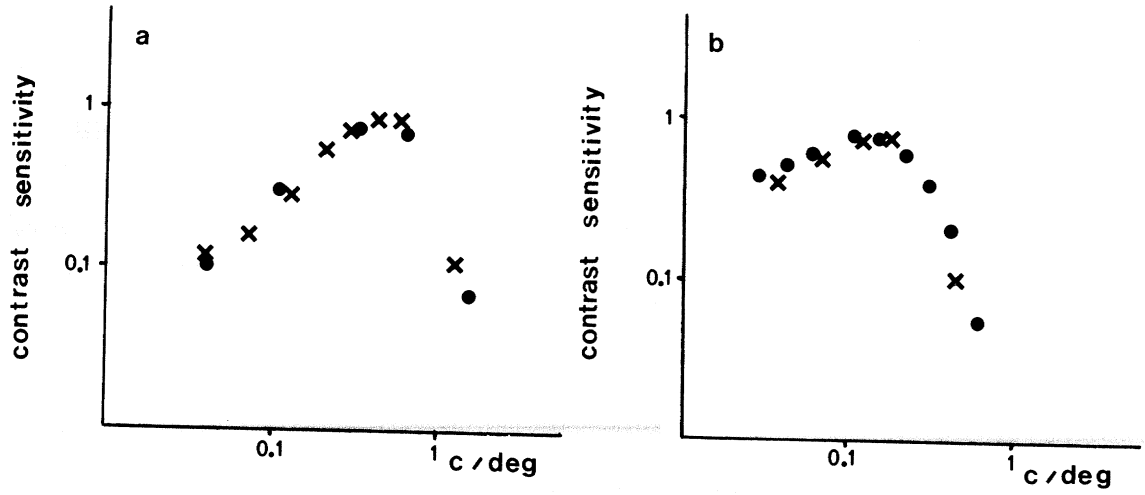

Figure 16. The response of X – and Y– ganglion cells to drifting sinusoidal grating. The simulated response to sinusoidal gratings of different spatial frequency, drifting at 4 Hz. (crosses), are compared with experimental results from the cat [Enroth-Cugell & Robson 1966] (circles), for X–type (a) and Y–type (b) units. Note that the contrast sensitivity curves do not tend to zero at zero frequency, although the receptive field is a ballanced DOG. This results in the model from the surround–center delay that induces some transient response even for a full field modulation. The higher low frequency response in the curve for Y–type units arises in the model not form a weaker"surround, but from the temporal differentiation. Abscissa – spatial frequency, ordinate – normalized response.

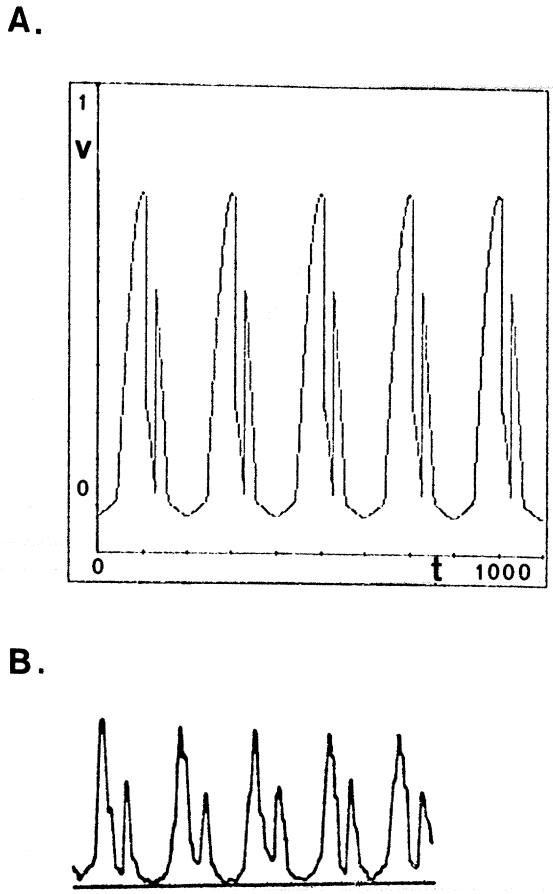

Figure 17. Response of an on-center Y-ganglion cell to a fast moving grating. The stimulus was a 0.1 c/w sinusoidal grating moving across the receptive field at a speed of 50 w/sec. The response was characterized by the on-dip (A) caused by the spike of the Amacrine cell. The recording in (B) is from a monkey [De Monasterio 1978 b, fig. 9] for a grating moving at a speed of about 50 w/sec. (10 deg./sec., w about 0.2 deg. wide). Calibration : Abscissa – time in milliseconds, Ordinate – relative response.

and of the inhibitory synapse as:

$$IN(t) = I\beta^2 \cdot te^{-\beta t}$$

The constants E and I are the amplification factors of the excitatory and inhibitory synapse, respectively. The potential change in the bipolar terminal is given by:

$$BP(T) = S(T) - \int_0^T AM(t) \cdot IN(T-t)dt$$

The potential change in the amacrine dendrite is:

$$AM(T) = \int_0^T BP(t) \cdot EX(T-t)dt$$

where BP(t) is the bipolar cell's potential, AM(t) the amacrine cell's potential, EX(t) the impulse response of the excitatory synapse, and IN(t) of the inhibitory one. The ganglion cell's potential change G(t) is produced by convolving the bipolar terminal signal BP(t) with the impulse response of the excitatory synapse to the ganglion cell:

$$G(t) = BP(t) * EX(t)$$

The final result of this calculation is shown in Figure 5-C.

Stability: In a linear feedback system complete transience and stability are opposing requirements. For a unit-step input, the steady-state response in the bipolar bipolar is $\frac{1}{1+IE}$. To achieve transience, the product IE has to be large, and this may cause instability in the systyem.

It turns out, however, that in the system described above both transience and stability can be achieved if the inhibitory response is sufficiently slower than the excitatory one. An analysis of the system's stability reveals that stability is maintained as long as the inequality $IE < \frac{(1+r)^2}{r}$ is satisfied, where $r = \frac{\alpha}{\beta}$. It is therefore possible in principle to achieve transience by making IE large, and avoid instability by increasing r.

The model used $r = 10$, which yields considerable transience, and at the same time the impulse response has only minor oscillations, that disappear in the transmission to the ganglion (see Fig. 5c).

Non-linearity: We have compared the linear model with the behaviour of a non-linear system, in which the inhibitory synapse changes the *Cl* conductance in the bipolar cell. For a number of stimuli we have examined (including short pulses and a step function), the results in the bipolar cell are quite similar to the linear model (For current injected into the amacrine cell the deviation is more significant where the nonlinear model predicts almost no response iin the bipolar cell while the linear one predicts some response in the bipolar.) . In the non-linear system it is possible to obtain a stable system with a higher degree of transience compared to the linear system.

4.3 Receptive field size in the man and monkey

The smallest DOG-shaped receptive field generated in the OPL has, according to the model, a center diameter of about 80" of arc. There are no direct data on the human retina to compare this estimate with. It is of interest, however, to compare this size with the available data from the rhesus.

Measurements from the rhesus monkey [De Monasterio, 1978a] show that the X units have an average "modal diameter" (the diameter at which the response of the center alone falls to 1/e of its peak response) of about 0.06 deg. (very likely an overestimation due to finite size of the stimulating spot, De Monasterio personal communication) For a DOG-shaped receptive field this would correspond to receptive fields about three times larger than the model's prediction. Taking into account the anatomical data (eyeball size ratio of about 2/3, similar cones size and spacing), Westheimer's reduced eye formula [Westheimer 1972, p. 461] predicts a scale factor of about 2.25 between the visual angle covered by a single cone, and consequently also between the corresponding receptive fields in the rhesus and human retinae. This formula is for an ideal optical system, abberation effects [Campbell & Gubisch, 1966] are expected to further increase the scale factor. We conclude that the measured receptive field sizes in the rhesus are not inconsistent with the smallest channel predicted by the model.

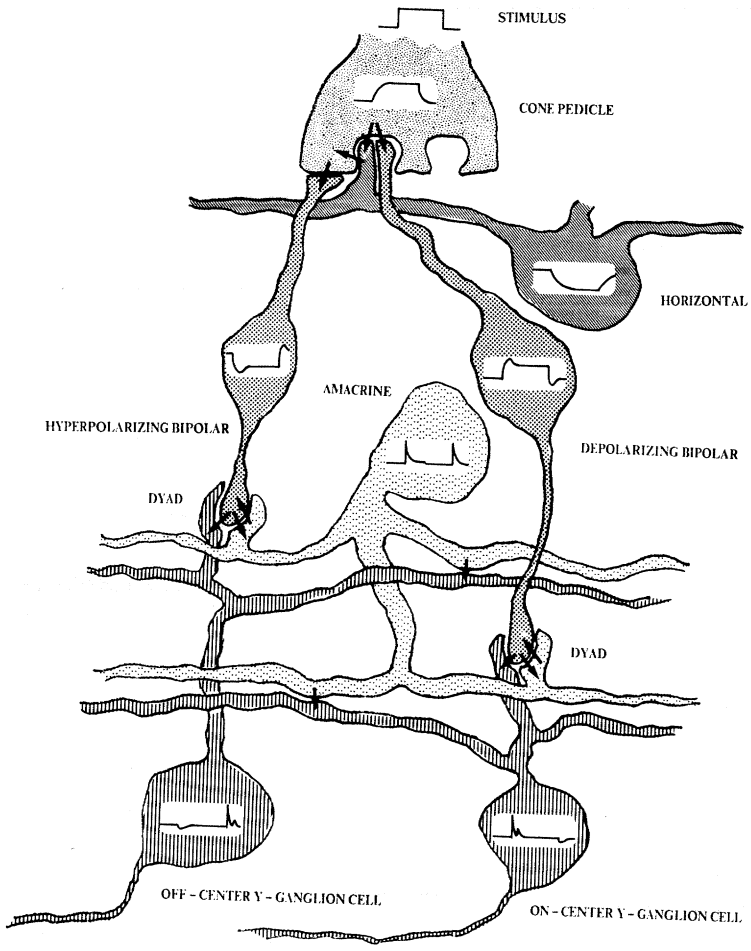

Figure 18. Functional and wiring model for a Y-ganglion cell in the retina. Schematic responses of the different cell types to a flashing spot of light, as predicted by the model, are shown inside the cells' somata. The arrows indicate the direction of transmission in the synapses. The synapses on the cone pedicle are the triad and the basal synapses and the three synapses at the efferent side of the bipolars are the dyad. The horizontal cell's efferent synapse may transmit to the bipolar cell rather than to the cone. The model refers to the primate's retina and in this respect the bipolar cells are flat bipolars (FB in figure 1),the amacrine is a bistratified amacrine cell and the ganglion cells are stratified ganglion cells (G4). [Boycott & Dowling 1969, fig. 98].

4.4 Flat bipolar cells and the formation of ganglion cell's receptive field.

Flat bipolar cells may be connected specifically only to cones of a single color population, thus forming color-coded units (similar to the midget bipolar cells). Alternatively, they may be connected to different color populations, giving rise to broad-band units. (Recent recordings from flat bipolar cells in the monkey [De Monasterio, personal communication) seem to support the second alternative.) The second case would imply that color-coded X channels are formed exclusively by midget bipolar cells. Different sizes of color-specific units may be then formed by convergence. It would therefore be of interest to investigate the color specificity of flat bipolar cells in primates.

4.6 Nonlinearity and convergence

According to the model, the rectification is introduced in the connection between bipolar cells and ganglion cells. In this scheme, the rectification by itself is insufficient to cause frequency doubling, since, if the cell's receptive field is not formed by converging subunits, its response will be nullified already at the linear bipolar cell's level. Thus, even if a midget ganglion cell has a rectified input from the bipolar cell, it would still exhibit a null position.

The Y-type receptive field was modeled by convergence of flat bipolars directly on the ganglion cell. This simple scheme is sufficient for the generation of the larger DOG-shaped field. However, different convergence schemes, e.g. using amacrine-to-amacrine interconnections cannot be ruled out.

4.7 Limitations of the model

The consideration of sufficiency is taken in dealing with the two main issues of this model. Thus it is demonstrated that spatial organization of the receptive field in the OPL is consistent with the anatomy of the retina and with recordings from bipolar cells, and no further organization is needed in the IPL to account for the ganglion cell's receptive field. It is also shown that the feedback mechanism in the dyad is sufficient for producing the derivative-like response of Y-cells. It is possible that the spatial organization or some part

of it is done in the IPL, and there are other ways to achieve derivative–like response that does not involve feedback mechanism.Our simulations does not exclude these possibilities. Nevertheless the model shows that there is enough computation capacity in the OPL for organizing the receptive field, and the analysis of the dyad throws some light on its performance whatever it is used for.

4.8 Implications of the model

The model has several implications to the retinal structure and physiology, and can be used to predict X- and Y-type responses to arbitrary spatio-temporal patterns.

4.8.1 Implications to retinal structure

There are several predictions regarding the retinal structure which, if disproved, will falsify important aspects of the model.

1. If the receptive field of midget bipolar cells is measured, it should have the final shape of the X-type unit, with a center diameter of about 80" of arc (about three times larger in the rhesus). Flat bipolar cells should have DOG-shaped receptive fields with a center size of about 150" (about 0.1 deg. in the rhesus).

2. The sign of the synapses should be positive for the bipolar-to-amacrine synapse, and negative for the amacrine-to-bipolar synapse.

3. The bipolar-amacrine interaction should be less efficient in X (sustained) units than in Y (transient) ones. That is, if the amacrine response to a stimulation in the bipolar cell, and the bipolar response to a stimulation in the amacrine cell, are measured, at least one of them, and possibly both, should be significantly less efficient in X-units than in Y-units.

4. If the bipolar-amacrine interaction can be blocked pharmacologically (e.g., by blocking the amacrine-to-bipolar inhibitory synapse), Y-units should become X-like (sustained) in their responses.

4.8.2 Predicting X- and Y-type responses

On the basis of the model, the X- and Y-type responses to arbitrary spatio-temporal patterns can be computed. We shall cite four examples.

1. The model predicts that the delay in the off response of an on-center Y unit to a flickering spot should

be significantly longer than the on response (see Section 3.2.2).

2. As mentioned in Section 3.3.2, it is predicted that at the exact center-surround boundary of a Y-unit, the on response to a flickering dot should be significantly larger than the off response (for an on-center unit). To obtain on and off responses of equal magnitudes, the flickering spot has to be displaced further towards the periphery.

3. The maximal response of pure X units to a moving grating is expected to depend on temporal frequency, and not on velocity. That is, for each grating, the velocity that induces a temporal frequency of about 6-8 Hz should give rise to a maximal response.

4. It should be possible to obtain a null position in a Y-unit for an alternating edge by employing a non-standard modulation of the edge. In the standard modulation, one half-field undergoes a positive intensity change, while the other half undergoes a negative change of equal magnitude. The model predicts that by making the positive change sufficiently smaller in amplitude compared to the negative one (a square wave modulation superimposed on the descending phase of a sawtooth intensity change), it would be possible to obtain a null response.

4.8.3 Implication to the relations among different X and Y properties

The model implies that certain X/Y properties are causally related.

Y-units have an on-off response to a flickering dot at the center-surround boundary (Section 3.2.2) as well as to an alternating edge (Section 2.4.2). According to the model, the first response is caused by the unit's transience (the derivative-like operation), and the second by the rectification. Any unit that shows a clear transience (e.g., to a spot in the middle of the receptive field) should necessarily give an on-off response to a flickering spot at the center-surround boundary. It may be possible, on the other hand, to find a transient but non-rectifying unit. Such a unit will still have the on-off response to a flickering spot at the center-surround boundary, but not to an alternating edge.

Acknowledgments.

We would like to thank B. Boycott, F.M. De Monasterio, J. E. Dowling, R. M. Shapley, V. Torre, M. J. Wright and G. Mitcheson for their invalueable comments J.R. is a research fellow in the center for cognitive science in M.I.T., and would like to thank the center and the Sloan Foundation for the invitation and the grant. This research was supported in part by the National Science Foundation Grant MCS77–07569.

Bibliography

Barlow H. B., Derrington A.M., Harris L. R. &Lennie P. (1977) The effect of remote retinal stimulation on the response of cat retinal ganglion cells. *J. Physiol. Lond. 269,* 177 - 194.

Baylor D. A. & Fettiplace R. (1979) Synaptic drive and impulse generation in ganglion cells of turtle retina. *J. Physiol Lond. 288,*107 - 127.

Baylor D. A. , Fourtes M. G. & O'Bryan P. M. (1971) Receptive fields of cones in the retina of the turtle. *J. Physiol. Lond. 214,* 265 - 294.

Baylor D. A. & Hodgkin A. L. (1973) Detection and resolution of visual stimuli by turtle photoreceptors. *J. Physiol. Lond. 234,* 163 - 198.

Boycott B. B. & Dowling J. E. (1969) Organization of the primate retina: light microscopy. *Phil. Trans. Roy. Soc. B 255,* 109 - 184.

Boycott B. B. & Kolb H. (1973) The horizontal cells of the rhesus monkey retina. *J. Comp. Neurol. 148,* 115 - 140.

Boycott B.B. & Wassle H. (1974) The morphological types of ganglion cells of the domestic cat's retina. *J. Physiol. Lond. 240,* 397 - 419.

Boycott B.B. , Dowling J.E. , Fisher S.K. , Kolb H. & Latis A. M. (1975) Interplexiform cells of the mammalian retina and their comparison with catecholamine – containing retinal cells. *Proc. Roy. Soc. B 191,* 353- 368.

Bullier J. & Norton T. T. (1979 a) X and Y relay cells in cat lateral geniculate nucleus : quantitative analysis of receptive field properties and classification. *J. Neurophysiol. 42,* 244 - 273.

Bullier J. & Norton T. T. (1979 b) Comparison of receptive field properties of X and Y ganglion cells with X and Y lateral geniculate cells in the cat. *J. Neurophysiol. 42,* 274 - 291.

Cajal S. R. (1911) ***Histologie du systeme nerveux de l'homme et des vertebres.*** vol. 2 Paris, Maloine.

Campbell F. W. & Gubisch R. W. (1966) Optical quality of the human eye. *J. Physiol. Lond. 186,* 558 -

578.

Chan R. Y. & Naka K-I (1976) The amacrine cell. *Vis. Res. 16,* 1119 - 1129.

Cleland B. G., Dubin M. W. & Levick W. R. (1971) Sustained and transient neurons in the cat's retina and LGN. *J. Physiol. Lond. 217,* 473 - 496.

Cleland B. G. & Levick W. R. (1974) Brisk and sluggish concentrically organized ganglion cells in the cat's retina. *J. Physiol. Lond. 240,* 421 - 456.

Cleland B. G. & Enroth - Cugell C. (1968) Quantitative aspects of sensitivity and summation in the cat retina. *J. Physiol. Lond. 198,* 17 - 38.

De Monasterio F. M. (1978 a) Properties of concentrically organized X and Y ganglion cells of macaque retina. *J. Neurophysiol. 41,* 1394 - 1417.

De Monasterio F. M. (1978 b) Center and surround mechanisms of opponent color X and Y ganglion cells of the retina of macaques. *J. Neurophysiol. 41,* 1418 - 1434.

De Monasterio F. M. & Gouras P. (1975) Functional properties of ganglion cells of the rhesus monkey retina. *J. Physiol. Lond. 251,* 167 - 195.

Dowling J. E. & Boycott B. B. (1966) Organization of the primate retina: electron microscopy. *Proc. R. Soc. Lond. B 166,* 80 - 111.

Dowling J. E. & Werblin F. S. (1969) Organization of the retina of the Mudpuppy *Necturus Maculosus* I : Synaptic structure. *J. Neurophysiol. 32,* 315 - 368.

Dreher B., Fukada Y. & Rodieck R. W. (1976) Identification classificaton and anatomical segregation of cells with X-like and Y-like properties in the LGN of old world primates. *J. Physiol. Lond. 258,* 433 - 452.

Dreher B. & Sanderson K. J. (1973) Receptive field analysis: Responses to moving visual contours by single lateral geniculate neurons in the cat. *J. Physiol. Lond. 234,* 95 - 118.

Dubin M. W. (1970) The inner plexiform layer of the vertebrate retina: a quantitative and comparative electron microscopic analysis. *J. Comp. Neurol. 140,* 479 - 506.

Enroth - Cugell C. & Robson J. G. (1966) The contrast sensitivity of retinal ganglion cells of the cat. *J. Physiol. Lond. 187,* 517 - 552.

Famiglietti E. V. Jr., Kaneko A. & Tachibana M. (1977) Neural architecture of on and off pathways to ganglion cells in carp retina. *Science 198,* 1267 - 1269.

Famiglietti E. V. Jr. & Kolb H. (1976) Structural basis for on and off center responses in retinal ganglion cells. *Science 194,* 193 - 195.

Fukada Y. & Stone J. (1974) Retinal distribution and central projections of Y-, X- and W- cellsof the cat's retina. *J. Neurophysiol. 37,* 749 - 772.

Hochstein S. & Shapley R. M. (1976 a) Quantitative analysis of retinal ganglion cell classifications. *J. Physiol. Lond. 262,* 237 - 264.

Hochstein S. & Shapley R. M. (1976 b) Linear and nonlinear spatial subunits in Y ; cat retinal ganglion cells. *J. Physiol. Lond. 262,* 265 - 284.

Hubel D. H. & Wiesel T. N. (1972) Laminar and columnar distribution of Geniculo - cortical fibers in the Macaque Monkey. *J. Comp. Neurol. 146,* 421 - 450.

Ikeda H. & Wright M.J. (1972) Receptive field organization of "sustained" and "transient" retinal ganglion cells which subserve different functional roles. *J. Physiol. Lond. 227,* 769 - 800.

Jack J. J. B., Noble D. & Tsien R. W. (1970) ***Electric current flow in excitable cells.*** Clarendon press, Oxford.

Kaneko A. (1970) Physiological and morphological identification of horizontal bipolar and amacrine cells in the gold fish. *J. Physiol. Lond. 207,* 623 - 633.

Kaneko A. (1971) Electrical connexions between horizontal cells in the gold fish retina. *J. Physiol. Lond. 213,* 95 - 105.

Kolb H. (1970) Organisation of the outer plexiform layer of the primates retina: electron microscopy of Golgi - impregnated cells. *Phil. Trans. Roy. Soc. B 258,* 261 - 283.

Kolb H., Boycott B.B. & Dowling J. E. (1969) A second type of midget bipolar cell in the primate retina.

Phil. Trans. Roy. Soc. B 255, 177 - 184.

Kolb H. , Mariani A. & Gallego A. (1980) A second type of horizontal cells in the monkey retina. *J. Comp. Neurol. 189*, 31 - 44.

Kuffler S. W. (1953) Discharge patterns and functional organization of mammalian retina. *J. Neurophysiol. 16,* 37 - 68.

Kuffler S. W. (1952) Neurons in the retina: organization , inhibition and excitation problems. *Cold Spring Harb. Symp. Quant. Biol. 17,* 281 - 292.

Kuffler S. W. & Nichols J. G. (1976) ***From neuron to brain.*** Sinauer associates inc. Sunderland Mass.

Marc R.E. & Sperling H.G. (1976) The chromatic organization of the gold fish cone mosaic. *Vis. Res. 16,* 1211 - 1224.

Marc R. E. & Sperling H.G. (1977) Chromatic organization of primate cones *Science 196* , 454 - 456.

Marchiafava P. L (1979) The responses of retinal ganglion cells to stationary and moving visual stimuli. *Vis. Res. 19,* 1203 - 1211.

Marchiafava P. L. & Torre V. (1978) The response of amacrine cells to light and intracellularly applied current. *J. Physiol. Lond. 276,* 83 - 102.

Mariani A. P. (1981) A diffuse, invaginating cone bipolar cell in primate retina. *J. Comp. Neurol. 197,* 661 - 671.

Marmarelis P. Z. & Naka K-I (1973) Nonlinear analysis and synthesis of receptive field responses in the catfish retina II. One input white noise analysis. *J. Neurophysiol. 36,* 619 - 633.

Marr D., Poggio T. & Hildreth E. (1980) Smallest channel in early human vision. *J. Opt. Soc. Am. 70,* 868 - 870.

Marr D. & Ullman S. (1980) Directional selectivity and its use in early visual processing. *Proc. Roy. Soc. , In the press.*

Miller R. F. & Dacheux R. F. (1976 a) Synaptic organization and ionic basis of on and off channels in mudpuppy retina. I: Intracellular analysis of chloride sensitive electrogenic properties of recep-

tors, horizontal cells, bipolar cells and amacrine cells. *J. Gen. Physiol. 67,* 639 - 659.

Miller R. F. & Dacheux R. F. (1976 b) Synaptic organization and ionic basis of on and off channels in mudpuppy retina. II: Chloride dependent ganglion cell mechanisms. *J. Gen. Physiol. 67,* 660 - 678.

Miller R. F. & Dacheux R. F. (1976 c) Synaptic organization and ionic basis of on and off channels in mudpuppy retina. III: A model of ganglion cell receptive field organization based on chloride free experiments. *J. Gen. Physiol. 67,* 679 - 690.

Naka K-I. (1972) The horizontal cell. *Vis. Res. 12,* 573 - 588.

Naka K-I. (1976) Neural circuitry in the catfish retina. *Invest. Opthal. 15,* 926 - 935.

Naka K-I & Witkovsky P. (1972) Dog fish ganglion cell discharge resulting from extrinsic polarization of the horizontal cells. *J. Physiol. Lond. 223,* 449 - 460.

Naka K-I., Marmarelis P. Z. & Chan R. I. (1975) Morphological and functional identification of catfish retinal neurons III functional identification. *J. Neurophysiol. 38,* 92 - 131.

Naka K-I & Nye P. W. (1970) Receptive field organization of the catfish retina: are at least two lateral mechanisms invovlved ? *J. Neurophysiol 33,* 625 - 642.

Naka K-I & Nye P. W. (1971) Role of horizontal cells in organization of the catfish retinal receptive field. *J. Neurophysiol. 34,* 785 - 801.

Nelson R. (1973) A comparison of electrical properties of neurons in *Necturus* retina. *J. Neurophysiol. 36* , 519 - 533.

Nelson R. (1977) Cat cones have rod input: A comparison of the response properties of cones and horizontal cell bodies in the retina of the cat. *J. Comp. Neurol. 172* , 109 - 136.

Nelson R. , Lutzow A. v. , Kolb H. & Gouras P. (1975) Horizontal cells in cat retina with independant dendritic systems. *Science 189* , 137 - 139.

Nelson R., Famiglietti E. V. Jr. & Kolb H. (1978) Intracellular staining reveals different levels of stratification for on and off center ganglion cells in cat retina. *J. Neurophysiol. 41,* 472 - 483.

Norton A. L., Spekreijse H., Wagner H. G. & Wolbarsht M.L. (1970) Responses to directional stimuli in retinal preganglionic units.*J. Physiol. Lond. 206,* 93 - 107.

O'Brien B. (1951) Vision and resolution in the central retina. *J. Opt. Soc. Am. 41,* 882 - 894.

Peichl L. & Wassle H. (1979) Size, scatter and coverage of ganglion cell receptive field centers in the cat retina. *J. Physiol. Lond. 291*, 117 - 141.

Polyak S. L. (1941) ***The retina.*** Chicago, University of Chicago press.

Polyak S. L. (1957) ***The vertebrate visual system.*** Chicago, University of chicago press.

Raviola E. (1976) Intercellular junctions inthe outer plexiform layer of the retina. *Invest. Ophtalmol. 15*, 881 - 895.

Rodieck R. W. (1965) Quantitative analysis of cat retinal ganglion cell response to visual stimuli. *Vis. Res. 5,* 583 - 601.

Rodieck R. W. (1973) ***The vertebrate retina. Principles of structure and function.*** San Francisco: Freeman.

Rodieck R. W. (1979) Visual pathways. *Ann. Rev. Neurosci. 2,* 193 - 225.

Rodieck R.W. & Stone J. (1965 a) Response of cat retinal ganglion cells to moving visual patterns. *J. Neurophysiol. 28,* 819 - 832.

Rodieck R.W. & Stone J. (1965 b) Analysis of receptive fields of cat retinal ganglion cells. *J. Neurophysiol. 28,* 833 - 849.

Shapley R.M. & Victor J.D. (1978) The effect of contrast on the transfer properties of cat retinal ganglion cells. *J. Physiol. Lond. 285,* 275 - 298.

Saito H. , Shimahara T. & Fukada Y. (1971) Phasic and tonic responses in the cat optic nerve fibers – stimulus - response relations. *Tohoku J. Exptl. Med. 104*, 313 - 323.

Schiller P. H. & Malpeli J. G. (1977) Properties and tectal projections of monkey retinal ganglion cells. *J. Neurophysiol. 40,* 428 - 445.

Scholes J. H. (1975) Colour receptors and their connections in the retina of a cyprinid fish. *Phil. Trans.*

Roy. Soc. B 270, 61 - 118.

Sherman S. M., Wilson J. R., Kaas J. H. & Webb S. V. (1976) X and Y-cells in the dorsal LGN of the owl monkey. *Science 192,* 475 - 477. Spekreijse H. (1969) Rectification in the Goldfish retina: analysis by sinusoidal and auxiliary stimulation. *Vis. Res. 9*, 1461 - 1472.

Stone J. & Hoffmann K. P. (1972) Very slow conducting ganglion cells in the cat's retina: A major, new functional type ? *Brain Res. 43*, 610 - 616.

Stone J. & Fukada Y. (1974) Properties of cat's ganglion cells: A comparison of W – cells with X – and Y – cells. *J. Neurophysiol. 37*, 722 - 748.

Van De Grind W. A., Grusser O. J. & Lunkenheimer W. R. (1973) Temporal transfer properties of the afferent visual system. Psychophysical, Neurophysiological and theoretical investigations. In ***Handbook of sensory physiology,*** vol. VII/3, ed. Jung R. Springer – Verlag, Berlin, Heidelberg, New - York.

Wassle H., Levick W. R. & Cleland B. G. (1975) The distribution of the alpha type of ganglion cells in the cat's retina. *J. Comp. Neurol. 159,* 419 - 438.

Wassle H. & Riemann H. J. (1978) The mosaic of nerve cells in the mammalian retina. *Proc. Roy. Soc. B 200,* 441 - 461.

Watson B. W. & Nachmias J. (1977) Patterns of temporal interaction in the detection of gratings. *Vis. Res. 17,* 893 - 902.

Werblin F. S. (1970) Response of retinal cells to moving spots: intracellular recording in necturus maculosus. *J. Neurophysiol. 33,* 342 - 350.

Werblin F. S. (1974) Control of retinal sensitivity II. Lateral interactions at the outer plexiform layer. *J. Gen. Physiol. 63,* 62 - 87.

Werblin F. S. (1977) Regenerative amacrine cell depolarization and formation of on-off ganglion cell response. *J. Physiol. Lond. 264,* 767 - 785.

Werblin F. S. & Dowling J. E. (1969) Organization of the retina of the mudpuppy *Necturus Maculosus*

II: Intracellular recording. *J Neurophysiol. 32,* 339 - 355.

Werblin F. S. & Copenhagen D. R. (1974) Control of retinal sensitivity III. Lateral interactins at the inner plexiform layer. *J. Gen. Physiol. 63,* 88 - 110.

Westheimer G. (1976) Diffraction theory and visual hyperacuity. *Am. J. Opt. and Physiol. optics 53,* 362 - 364.

Wunk D.F. & Werblin F. S. (1979) Synaptic input to the ganglion cells in the tiger salamander retina.*J. Gen. Physiol. 73,* 265 - 286.